

# Magnetic Fields, Relativistic Particles, and Shock Waves in Cluster Outskirts

Marcus Brüggen · Andrei Bykov ·  
Dongsu Ryu · Huub Röttgering

Received: date / Accepted: date

**Abstract** It is only now, with low-frequency radio telescopes, long exposures with high-resolution X-ray satellites and  $\gamma$ -ray telescopes, that we are beginning to learn about the physics in the periphery of galaxy clusters. In the coming years, Sunyaev-Zeldovich telescopes are going to deliver further great insights into the plasma physics of these special regions in the Universe. The last years have already shown tremendous progress with detections of shocks, estimates of magnetic field strengths and constraints on the particle acceleration efficiency. X-ray observations have revealed shock fronts in cluster outskirts which have allowed inferences about the microphysical structure of shocks fronts in such extreme environments. The best indications for magnetic fields and relativistic particles in cluster outskirts come from observations of so-called radio relics, which are megaparsec-sized regions of radio emission from the edges of galaxy clusters. As these are difficult to detect due to their low surface brightness, only few of these objects are known. But they have provided unprecedented evidence for the acceleration of relativistic particles at shock fronts and the existence of  $\mu\text{G}$  strength fields as far out as the virial radius of clusters. In this review we summarise the observational

---

Marcus Brüggen  
Jacobs University Bremen, Campus Ring 1, 28759 Bremen, Germany, E-mail:  
m.brueggen@jacobs-university.de

Andrei M. Bykov  
Ioffe Institute for Physics and Technology, 194021 St.Petersburg, Russia, E-mail:  
byk@astro.ioffe.ru

Dongsu Ryu  
Department of Astronomy and Space Science, Chungnam National University, Dae-jeon 305-764, Korea, E-mail: ryu@canopus.cnu.ac.kr

Huub Röttgering  
Leiden Observatory, Leiden University, P.O. Box 9513, NL-2300 RA, Leiden, The Netherlands, E-mail: rottgering@strw.leidenuniv.nl

---

and theoretical state of our knowledge of magnetic fields, relativistic particles and shocks in cluster outskirts.

**Keywords** ...

## 1 Introduction

Clusters of galaxies are filled with a dilute ( $n_e \leq 0.1 \text{ cm}^{-3}$ ), hot ( $T > 10^7 \text{ K}$ ) gas, the so-called intracluster medium (ICM). In this review, we are primarily concerned with regions outside of cluster cores, close to the virial radius ( $\sim 1 \text{ Mpc}$ ). The ICM contains the majority of baryons in galaxy clusters and has a temperature close to the virial temperature of the gravitational potential of the cluster.

Shocks play a fundamental role in the evolution of the ICM and affect clusters in two ways: First, shocks thermalize the incoming gas allowing it to virialise and providing much of the pressure support in baryons. Secondly, because these shocks are collisionless features whose interactions in the hot plasma are mediated by electromagnetic fields, it is possible for a fraction of the thermal distribution of particles to be accelerated and transformed into nonthermal populations of cosmic rays (CRs) through diffusive shock acceleration. This process results in a part of the kinetic energy to be converted to non-thermal components. Non-thermal populations of particles can in principle be observed in the hard X-rays through inverse Compton scattering of the Cosmic Microwave background, in the gamma-rays through hadronic interactions of non-thermal protons with the thermal component and in the radio band through synchrotron radiation of the electrons. The latter has been observed in galaxy clusters in the form of diffuse radio sources. These sources are usually subdivided into two classes, denoted as 'radio haloes' and 'radio relics' (see e.g. Ferrari et al. (2008) for a review).

Radio haloes are diffuse, low surface brightness ( $\simeq 10^{-6} \text{ Jy/arcsec}^2$  at 1.4 GHz), steep-spectrum<sup>1</sup> ( $\alpha > 1$ ) sources, permeating the central regions of clusters, produced by synchrotron radiation of relativistic electrons with energies of  $\simeq 10 \text{ GeV}$  in magnetic fields with  $B \simeq 0.5 - 1 \mu\text{G}$ . Radio haloes represent the best evidence for the presence of large-scale magnetic fields and relativistic particles throughout the intra-cluster medium (ICM). They are mostly unpolarized and have diffuse morphologies that are similar to those of the thermal X-ray emission of the cluster gas. Their origin and the role that shocks play in their formation are still subject to debate, (see e.g., Petrosian and Bykov 2008, Petrosian et al. 2008, Brunetti et al. 2009, for recent review). Unlike haloes, radio relics are typically located near the periphery of the cluster. They often exhibit sharp emission edges and many of them show strong radio polarization. For some relics there is now good evidence that these electrons are produced by shock waves and we will present this evidence in Sec. 4.

If a significant fraction of the pressure of the ICM is provided by CRs, this will affect gas mass fraction estimates. Since gas mass fractions in clusters

---

<sup>1</sup>  $S(\nu) \propto \nu^{-\alpha}$

are used to make inferences about dark energy, a knowledge about the non-thermal content of galaxy clusters is important for their use in precision cosmology (e.g. Vikhlinin et al. 2010).

There are three types of phenomena that create shocks in the ICM. The first class of shocks are accretion shocks: At very large off-center distances, typically several Mpc, cosmological simulations predict that intergalactic medium (IGM) continues to accrete onto the clusters through a system of shocks that separate the IGM from the hot, mostly virialized inner regions. The IGM is much cooler than the ICM, so these accretion (or infall) shocks should be strong, with Mach numbers  $M \sim 10 - 100$  (e.g., Bertschinger 1984, Zeldovich 1972, Miniati et al. 2000). As such, they were suggested as sites of effective cosmic ray acceleration, with consequences for the cluster energy budget and the cosmic gamma-ray background.

The second class of shocks are merger shocks: as subhalos fall into the main clusters, they create moderate-strength shocks that allow the gas to virialise. If an infalling subcluster has a deep enough gravitational potential to retain at least some of its gas when it enters the dense, X-ray bright region of the cluster into which it is falling, a merger shock is produced. In Sec. 2, we will discuss some prominent observations of this type of shocks.

The third class of shocks are AGN shocks: Powerful AGN are observed to inflate large bubbles in the ICM, which may generate shocks within the central few hundred kiloparsecs (Brüggen et al. 2007, Simionescu et al. 2009). Like merger shocks, these shocks have moderate Mach numbers, and have been detected in cluster centres, such as in Virgo and Hydra A. These shocks are very important because they convert the energy produced by the central supermassive black hole into thermal energy and, thus, complete the feedback loop which is regarded as essential for galaxy evolution (Cattaneo et al. 2009). As these shocks are primarily found in cluster centres, they will not be the subject of this review.

The setup of this review is as follows: In Sec. 2, we introduce some phenomena that we will cover in this review and explain some basic terms. In Sec. 3, we describe our current knowledge of cluster shocks from X-ray and  $\gamma$ -ray observations. Then we summarise what we can learn from radio observations in Sec. 4, including estimates of magnetic fields in cluster outskirts from recent observations of radio relics. In Sec. 5, we review recent results concerning structure formation shocks from cosmological simulations. In Sec. 6, we then discuss the origin of magnetic fields and relativistic particles in shocks. Finally, in Sec. 7, we summarise insights gained in the last years on the physics of shocks in such dilute environments as found in cluster outskirts and identify open questions.

## 2 Fundamentals

**Shock structure:** Shock waves are usually regarded as a sharp transition between a supersonic (and super-Alfvénic) upstream flow and a subsonic downstream flow. In a rarefied hot cosmic plasma the Coulomb collisions are not sufficient to provide the viscous dissipation of the incoming flow, and collective effects due to the plasma flow instabilities play a major role. Hence,

---

cosmological shocks in a rarefied highly ionised plasma are collisionless. Protons, whose thermal velocity is lower than the shock velocity, are heated dissipatively at the shock layer. However, the equilibration of electrons may differ substantially from that of the ions because of their smaller gyroradii. The amount of collisionless heating of electrons depends on the shock velocity and the Mach number (see e.g. Schwartz et al. 1988, Bykov and Uvarov 1999). Then the Coulomb equilibration eventually occurs on scales that are orders of magnitude longer than the collisionless heating scale length (see e.g. Fox and Loeb 1997, Bykov et al. 2008b). Under such circumstances, the shock structure can be more complex because electrons and ions can remain out of equilibrium for a while. Then such a shock consists of an ion viscous jump and an electron-ion thermal relaxation zone. We will revisit the microphysics of cluster shocks in Sec. 6.

**Shock acceleration:** Shocks can also change the momentum distribution of a gas by accelerating a fraction of the particles to very high energies. This has been observed in astrophysical shocks on a wide range of scales. Examples are the shock waves that form when the solar wind collides with planetary magnetospheres, shocks surrounding supernova remnants in the interstellar medium and shocks in active, extragalactic sources such as quasars and radio galaxies. The resulting energies reach up to about 100 keV in the shock in the Earth’s magnetosphere to about 100 TeV in supernova remnants. Particles gain energy whenever they cross the shock front in either direction. Scattering processes make the velocity distribution isotropic with respect to the local rest frame on either side of the shock front. Consequently, there is a certain probability that a particle that has just gone through the shock and been accelerated will diffuse back through the shock to where it came from. Every time the particle crosses the shock it will gain energy. Moreover, the increase in energy is the same no matter from which direction the particle crosses the (non-relativistic) shock. Particle passing back and forth through the shock can thus attain very high energies. This process is called first-order Fermi (Fermi-I) acceleration or diffusive shock acceleration (DSA; Krymskii 1977, Axford et al. 1977, Bell 1978a,b, Blandford and Ostriker 1978, Drury 1983, Blandford and Eichler 1987, Jones and Ellison 1991, Malkov and O’C Drury 2001). The cosmic rays thus generated can penetrate far into the upstream flow, thus creating a shock precursor. The particles decelerate the flow and preheat the gas. If the cosmic ray pressure inside the shock becomes comparable to the thermal pressure, the cosmic rays will also modify the structure of the shock. Finally, shocks can efficiently generate strong fluctuating magnetic fields in the upstream region due to cosmic-ray driven instabilities (Bell 2004, Bykov et al. 2011).

**Cluster magnetic fields:** The origin of magnetic fields in galaxy clusters remains unclear (see e.g. Dolag et al. (2008) for a review). It has been suggested that they are primordial; i.e., a seed field that has formed prior to recombination is subsequently amplified by compression and turbulence. Alternatively, it has been proposed that the magnetic field is of proto-galactic origin (Kulsrud et al. 1997, Ryu et al. 2008) or that it had been produced

---

by a cluster dynamo (Roettiger et al. 1999). Others conclude that magnetic fields can be produced efficiently in shocks by the Weibel instability (Medvedev et al. 2004) or by small-scale plasma instabilities (Schekochihin et al. 2005). Finally, it has been suggested that the intergalactic medium has been magnetised by bubbles of radio plasma that are ejected by active galactic nuclei (Furlanetto and Loeb 2001). Cluster magnetic fields are the subject of a separate chapter in this review and in this review we will focus on magnetic fields in cluster outskirts only.

**Turbulence:** Mergers, the motions of galaxies and the action of AGN produce turbulence in the ICM. Turbulence may have a deep impact on the physics of the ICM (see e.g. Schekochihin et al. 2005, Lazarian 2006) and on the properties of non-thermal components in galaxy clusters (see e.g. Brunetti and Lazarian 2011). The presence of turbulent gas motions in the ICM is suggested by measurements of the Faraday Rotation of the polarization angle of the synchrotron emission from cluster radio galaxies. These studies show that the magnetic field in the ICM is tangled on a broad range of spatial scales (see e.g. Vogt and Enßlin 2005) suggesting the presence of super-Alfvénic motions in the medium. Also independent attempts from X-ray observations of a number of nearby clusters, based on pseudo-pressure maps of cluster cores and on the lack of evidence for resonant scattering effects in the X-ray spectra, provide hints of turbulence in the ICM (see e.g. Churazov et al. 2004). Important constraints on the fraction of the turbulent and thermal energy in the cores of clusters are based on the analysis of line broadening in the emitted X-ray spectra of cool core clusters (Sanders et al. 2010). In the outskirts of clusters, simulations predict that the turbulent pressure support increases relative to the thermal pressure support (Vazza et al. 2010, Paul et al. 2010, Nagai and Lau 2011).

### 3 Cluster shocks in X- and $\gamma$ -ray emission

#### 3.1 Cluster shocks in X-rays

Regions of high-entropy gas in clusters have been observed by *ROSAT*, *ASCA*, *XMM-Newton* and *Chandra* and have been interpreted as the result of shock heating (e.g., Belsole et al. 2005). However, only a handful of shock fronts, exhibiting both a sharp gas density edge and an unambiguous temperature jump, have been found: in the "bullet cluster", 1E 065756 (Markevitch et al. 2002), Abell 520 (Markevitch et al. 2005), and Abell 2146 (Russell et al. 2010). Such discoveries are so rare because one has to observe a merger when the shock has not yet moved to the low-brightness outskirts, and is propagating nearly in the plane of the sky, to give us a clear view of the shock discontinuity. In addition, the shocks in A520 and 1E 065756 have Mach numbers of  $M \sim 2-3$ , which provide a big enough gas density jump to enable accurate deprojection. Merger shock fronts have been found in other clusters, e.g., in A3667, (Finoguenov et al. 2010), A754, (Krivonos et al. 2003), A521, (Giacintucci et al. 2008).

Recently, Finoguenov et al. (2010) analysed *XMM-Newton* and *Suzaku* pointings of the cluster Abell 3667, including the NW relic (see Fig. 1). They find a sharp X-ray surface brightness discontinuity at the outer edge of the radio relic, and a significant drop in the hardness of the X-ray emission at the same location. This discontinuity is consistent with a Mach number 2 shock moving at 1200 km/s associated with the merger. Kinetic energy is being dissipated in this shock at a rate of  $dE_{\text{KE}}/dt \sim 1.8 \times 10^{45}$  erg/s. The total non-thermal luminosity of the relic is  $L_{\text{NT}} \approx 3.8 \times 10^{42} [(3.6 \mu\text{G}/B)^2 + 1]$  erg  $\text{s}^{-1}$ . If this energy is provided by the shock acceleration of electrons, then a fraction  $\epsilon \sim 0.2$  % of the kinetic energy flux through the shock is converted to the non-thermal luminosity. Shock acceleration at the outer edge of the relic and radiative losses as the electrons are advected away from the shock can explain the rapid steepening of the radio spectral index with distance from this edge of the relic. Alternatively, the surface brightness discontinuity and hardening of the X-ray spectrum might be due to Inverse Compton (IC) emission from the relic. In this case, the magnetic field in the relic is about  $3 \mu\text{G}$ . Since the observed X-ray excess from the relic is an upper limit to IC emission, this yields a lower limit on the relic magnetic field of  $\geq 3 \mu\text{G}$ . This is a remarkably strong magnetic field at this large projected distance (2.2 Mpc) from the cluster center, but is consistent with Faraday rotation through the relic observed towards two background radio galaxies.

The bow shock in 1E 065756 offers a unique experimental setup to determine how long it takes for post-shock electrons to come into thermal equilibrium with protons in the ICM (Markevitch et al. 2006). Currently, X-ray observations only yield the electron temperature but not the ion temperature. However, one can use the measured gas density jump at the shock front and the pre-shock electron temperature to predict the post-shock adiabatic and instant-equilibration electron temperatures, using the adiabatic and the Rankine-Hugoniot jump conditions, respectively, and compare them with the data. Furthermore, if the downstream velocity of the shocked gas flowing away from the shock is known, one can deduce how the flow spreads out the electron temperature along the spatial coordinate in the plane of the sky. The Mach number of the 1E 065756 shock is sufficiently high, such that the adiabatic and shock electron temperatures are sufficiently different (for  $M \leq 2$ , they become close and difficult to distinguish, given the temperature uncertainties). Moreover, the distance traveled by the post-shock gas during the time, is well-resolved by *Chandra*. Markevitch et al. (2006) found that the temperatures are consistent with instant heating; equilibration on the collisional timescale is excluded, although with a relatively low 95% confidence. The equilibration timescale should be at least 5 times shorter than the Coulomb time. We will revisit the theory of dissipation in collisionless shocks in Sec. 6.

The low surface brightness of the cluster outskirts is challenging for current X-ray telescopes (e.g. Böhringer and Werner 2010, Ettori and Molendi 2010). Projected temperature profiles to  $\sim 0.5r_{200}$  of 15 nearby ( $z < 0.2$ ) clusters were derived from *XMM-Newton* observations by Pratt et al. (2007) (see also Vikhlinin et al. 2005).

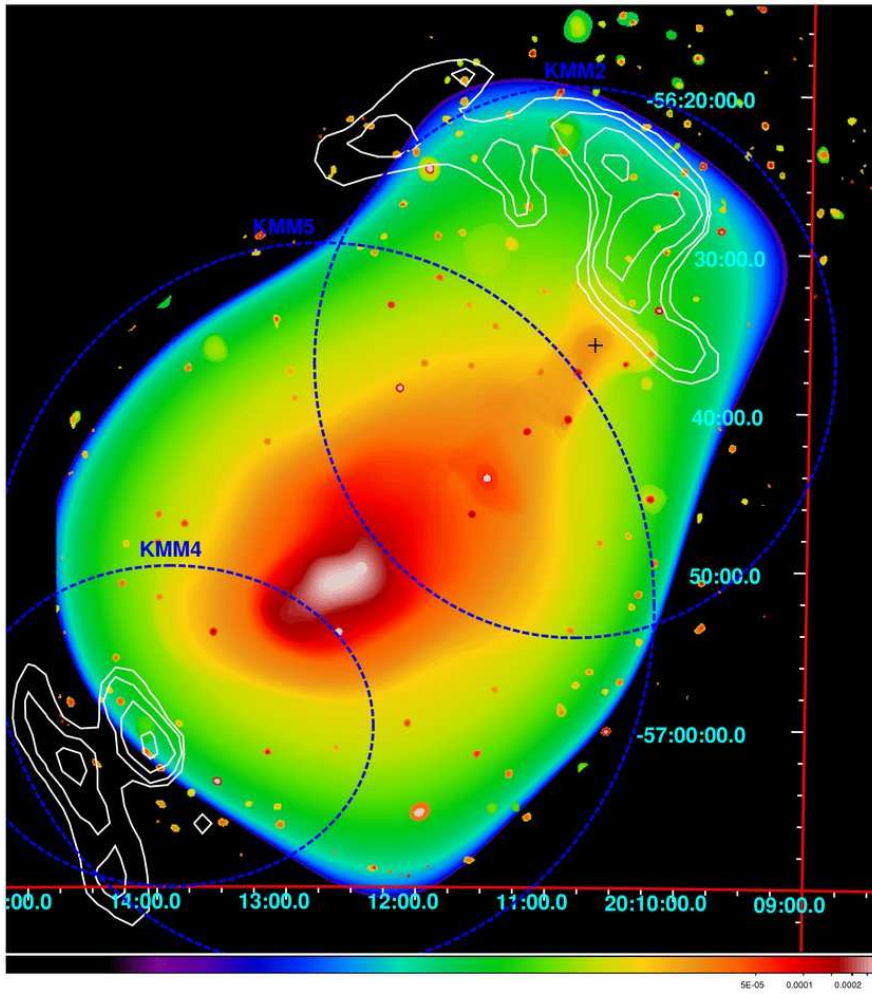


**Fig. 1** Wavelet reconstruction of the 0.5-2 keV X-ray mosaic of A3667 from *XMM-Newton*. There is a sharp discontinuity in the X-ray surface brightness to the NW; the blue ellipses show the location, name and size of three main galaxy components (KMM5, KMM2, and KMM4) of A3667 from the analysis of Owers et al. (2009). The black cross marks the center of KMM2 group. The white contours show the wavelet reconstruction of the SUMMS 843 MHz radio image in the region of radio relics. The contours are drawn at the 1, 3, 9, and 20 mJy/beam levels. From Finoguenov et al. (2010) with kind permission.

The low and well-constrained background levels make *Suzaku* the prime instrument for the study of X-ray emission from cluster outskirts. *Suzaku* is in a low orbit within Earth's magnetopause providing significantly lower and stable particle background compared to *Chandra* and *XMM-Newton*. However, the calibration of the instruments can sometimes be difficult. The low surface brightness outskirts of A2204 around  $r_{200}$  were studied by Reiprich et al. (2009) with *Suzaku*. Simionescu et al. (2011) determined ICM properties out

to the edge of the Perseus Cluster. Contrary to earlier findings, the cluster baryon fraction is consistent with the expected universal value at half of the virial radius. The apparent baryon fraction exceeds the cosmic mean at larger radii, suggesting a clumpy distribution of the gas for radii larger than half of the virial radius. Also with *Suzaku*, George et al. (2009) studied X-ray emission from the outskirts of the cluster of galaxies PKS 0745-191 at  $z = 0.1028$ . They determined radial profiles of density, temperature, entropy, gas fraction, and mass beyond the virial radius out to  $\sim 1.5r_{200}$ . The temperature is found to decrease by roughly 70 % from 0.3-1  $r_{200}$ . *Suzaku* observations provide evidence for departure from hydrostatic equilibrium around and even before the virial radius as it is seen in the galaxy cluster Abell 1795 (e.g. Bautz et al. 2009). *Suzaku* observations of PKS 0745-191 revealed one shock front possibly indicating that this cluster is still accreting material, likely along a filament. Evidence for nonthermal pressure support suggests that bulk motions from merger activity could be making a significant contribution to the gas energy in the outskirts of this cluster (George et al. 2009). There is some evidence for the presence of an excess above the dominating thermal emission of the ICM hot gas in both X-rays and EUV (Rephaeli et al. 2008, Durret et al. 2008, Million and Allen 2009). However, a recent search by Ajello et al. (2009) of hard X-ray excess above the thermal emission in a large sample of clusters with *Swift Burst Alert Telescope* does not show significant nonthermal hard X-ray emission. The only exception is Perseus whose high-energy emission Ajello et al. (2009) attributed to the central galaxy NGC 1275. In the next years, as more cluster outskirts are being observed with *Suzaku*, more conclusive results on shocks and nonthermal components are expected.

Compared to X-ray observations, the outer regions of clusters can potentially be better studied by Sunyaev-Zel'dovich (SZ) observations because the SZ effect depends only on the electron density to the first power, while the X-ray emission depends on the electron density squared. Facilities such as the Atacama Cosmology Telescope (ACT), the South Pole Telescope (SPT) and the Planck satellite are searching for the SZ signal of galaxy clusters and have found some interesting first results. For example, it was found that the SZ signal caused by clusters is by a factor of  $\sim 2$  smaller than predicted by models of clusters that suggest that the pressure by the electrons has been overpredicted Lueker et al. (2010). This is presumably caused by a substantial nonthermal pressure at cluster outskirts, most of it is likely to be turbulent pressure (see e.g. Shaw et al. 2010). This picture is also supported by simulations (Vazza et al. 2010, Paul et al. 2010, Nagai and Lau 2011) which we review in Sec. 5.

Given the advancements in the X-ray and SZ observations of the cluster outer regions, as well as the growing evidence of missing thermal energy in the ICM and the possible negative implications for cosmological tests, a more detailed study of the kinetic processes in cluster envelopes is necessary.

### 3.2 $\gamma$ -ray Observations

Recently, Ackermann et al. (2010) reported on the search for GeV emission from clusters of galaxies using the *Large Area Telescope* on the *Fermi*



*Gamma-ray Space Telescope*. Only upper limits on the photon flux were reported in the range 0.2-100 GeV toward a sample of around 30 observed clusters (typical values  $(1 - 5) \times 10^{-9}$  ph cm $^{-2}$  s $^{-1}$ ), considering both point-like and spatially resolved models for the high-energy emission. The authors concluded that the volume-averaged relativistic hadron-to-thermal energy density ratio is below 5% – 10% in several clusters. Also, using *High Energy Stereoscopic System (H.E.S.S.)* observations of Coma cluster, Aharonian et al. (2009) placed an upper limit  $\sim 10^{-13}$  ph cm $^{-2}$  s $^{-1}$  at photon energies above 5 TeV for the Coma core of 0.2 degrees in radius constraining the multi-TeV particle population in the cluster. In summary, at this time the  $\gamma$ -ray observations remain inconclusive with respect to the origin of diffuse radio emission in clusters, but this is bound to change soon as the upper limits are expected to decrease.

#### 4 Cluster shocks in radio emission

A number of diffuse, steep-spectrum radio sources without optical identification have been observed in galaxy clusters. The emission from these sources is synchrotron radiation, which indicates the presence of highly relativistic electrons and  $\mu$ G range magnetic fields. Especially radio relics are thought to trace cosmological shocks. Radio relics can be divided into two main groups (Kempner et al. 2004). *Radio gischt* are large elongated, often Mpc-sized, radio sources located in the periphery of merging clusters. They probably trace shock fronts in which particles are accelerated via the diffusive shock acceleration mechanism. Among them are double-relics with the two relics located on both sides of a cluster center (e.g., Bonafede et al. 2009, van Weeren et al. 2009b, Venturi et al. 2007, Bagchi et al. 2006, Röttgering et al. 1997). According to DSA, the integrated radio spectrum should follow a single power-law. *Radio phoenixes* are related to radio-loud AGN. Fossil radio plasma from a previous episode of AGN activity is thought to be compressed by a merger shock wave which boosts, both, the magnetic field inside the plasma as well as the momenta of the relativistic particles. As a result the radio plasma brightens in synchrotron emission. In contrast to the radio gischt, the phoenixes have a steep curved spectrum<sup>2</sup> indicating an aged population of electrons.

The sizes of relics and the distance to the cluster centre vary significantly. Examples for radio relics with sizes of 1 Mpc or even larger have been observed in Coma (the prototype relic source 1253 + 275, (Giovannini et al. 1991), Abell 2255 (Feretti et al. 1997) and Abell 2256 (Rottgering et al. 1994), which contain both a relic and a halo (as do Abell 225, Abell 521, Abell 754, Abell 1300, Abell 2255 and Abell 2744). The cluster Abell 3667 contains two very luminous, almost symmetric relics with a separation of more than 5 Mpc (Rottgering et al. 1997), as does ZwCl 2341.1+0000 (van Weeren et al. 2009c, Giovannini et al. 2010), and Abell 2345 and Abell 1240 (Bonafede et al. 2009). The clusters A115 and A1664 show relics only at one side of the elongated X-ray distribution (Govoni et al. 2001). Recently, another double radio relic

---

<sup>2</sup>  $F_\nu \propto \nu^\alpha$ , with  $\alpha$  the spectral index

was found in the galaxy cluster ZwCl 0008.8+5215 (van Weeren et al. 2010) which we will discuss in detail below.

The relic with the best evidence for shock acceleration found to date is located in the northern outskirts of the merging galaxy cluster CIZA J2242.8+5301 ( $z = 0.1921$ ), see Fig. 2. The relic is located at a distance of 1.5 Mpc from the cluster center and spans 2 Mpc in length. The relic shows a clear unambiguous spectral index gradient towards the cluster center. The spectral index, measured between 2.3 and 0.61 GHz, steepens from  $-0.6$  to  $-2.0$  across the width of the narrow relic. The gradient is visible over the entire 2 Mpc length of the relic, something that has never been observed before. This is a crucial observation as it constitutes clear evidence for diffusive shock acceleration and spectral ageing of relativistic electrons in an outward moving shock. The relic is strongly polarized at the 50-60% level, indicating an ordered magnetic field, and polarization magnetic field vectors are aligned with the relic (see Fig. 3). In the southern part of the cluster a second fainter broader relic is found and the elongated radio relics are orientated perpendicular to the major axis of the cluster's elongated ICM. This is exactly as expected for a binary cluster merger event in which this second southern relic traces the shock wave that travels in the opposite direction from the first one. Furthermore, a faint halo of diffuse radio emission is seen extending all the way towards the cluster center connecting the two radio relics. This emission extends over 3.1 Mpc, making it by far the largest known diffuse radio source in a cluster to date.

The spectral index at the front of the relic is  $\alpha = -0.6 \pm 0.05$ . In simple shock acceleration theory,  $\alpha$  is related to the Mach number via  $\alpha = -(3 + M^2)/(2M^2 - 1)$  (Rosswog and Bruggen 2007), which yields a Mach number of  $4.6_{-0.9}^{+1.3}$ . Subsequent hydrodynamic simulations of this shock front have indicated slightly lower Mach number of around 3. Using the  $L_X - T$  scaling relation for clusters (Markevitch 1998), we estimate the average temperature of the ICM to be  $\sim 9$  keV. Behind the shock front the temperature is likely to be higher. Using the redshift, downstream velocity, spectral index, and characteristic synchrotron timescale, the width of the relic is given by

$$l_{\text{relic}} \approx 110 \text{ kpc} \times \frac{B^{1/2} B_{\text{CMB}}^{3/2}}{B^2 + B_{\text{CMB}}^2} \quad (1)$$

for a relic seen edge-on without any projection effects.  $B_{\text{CMB}}$  is the equivalent field strength of the IC scattering from the Cosmic Microwave Background, which is known, and thus the measurement of  $l_{\text{relic}}$  from the radio maps, directly constrains the magnetic field. From the 610 MHz image (the image with the best signal to noise ratio and highest angular resolution), the relic has a deconvolved width (FWHM) of 55 kpc. Taking into account projection effects, van Weeren et al. (2010) conclude that the magnetic field strength at the location of the bright radio relic lies between 5 and 7  $\mu\text{G}$ . As in A3667, this measurement points towards  $\mu\text{G}$ -scale fields in merger shocks found at large distances from the cluster centre.

Even though the sample of known radio relics is still small, one can start to find correlations between size, location and spectral index of these unique sources, which can eventually be compared to simulations of relic formation.

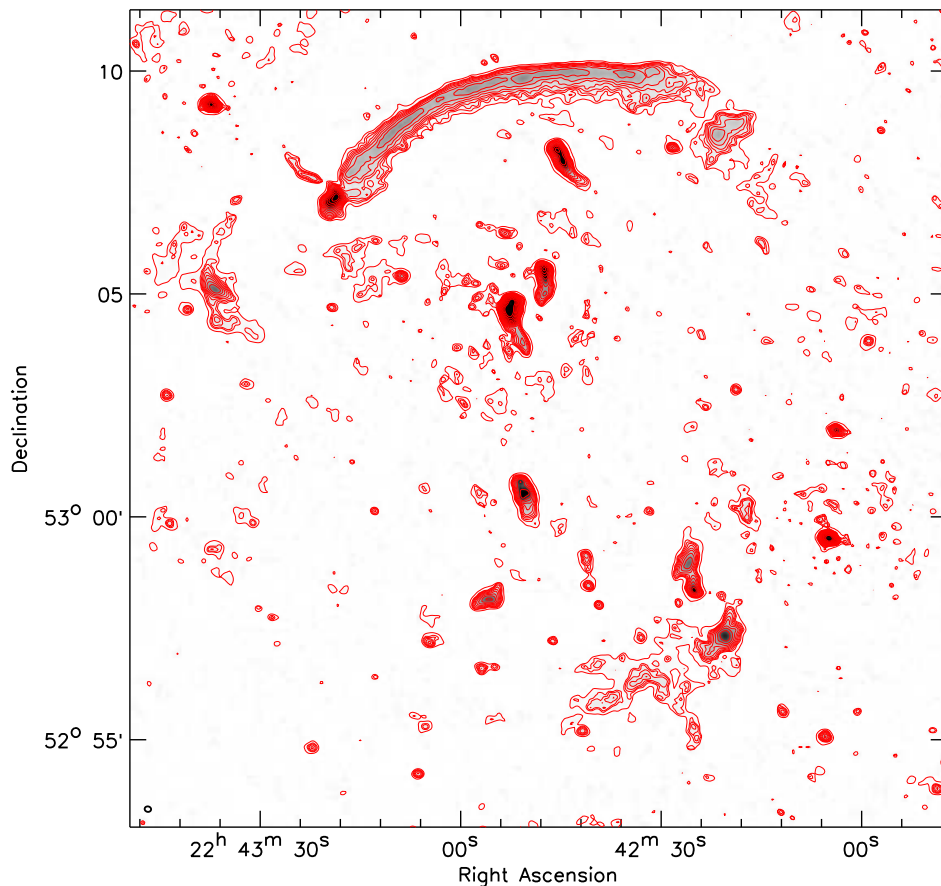


**Fig. 2** Radio map (GMRT 325 MHz) of the relic in CIZA J2242.8+5301. From van Weeren et al. (2010).

The spectral index of the radio relics, versus the physical size is shown in Fig. 4. The projected distance from the cluster center is color coded. Van Weeren et al. (2010) find that on average the smaller relics have steeper spectra. Such a trend is in line with predictions from shock statistics derived from cosmological simulations (Skillman et al. 2008, Battaglia et al. 2009, Hoeft et al. 2008). They find that larger shock waves occur mainly in lower-density regions and have larger Mach numbers, and consequently shallower spectra. Conversely, smaller shock waves are more likely to be found in cluster centers and have lower Mach numbers and steeper spectra. We note that more spectral index measurements of high quality are needed to confirm the correlation between physical size and spectral index.

A further confirmation of the binary merger origin of most radio relics comes from measuring the angle of orientation of the relic's main axis with respect to the major axis of the X-ray surface brightness map of the host cluster. We have computed the angle  $\alpha$  between the major axis of the ICM

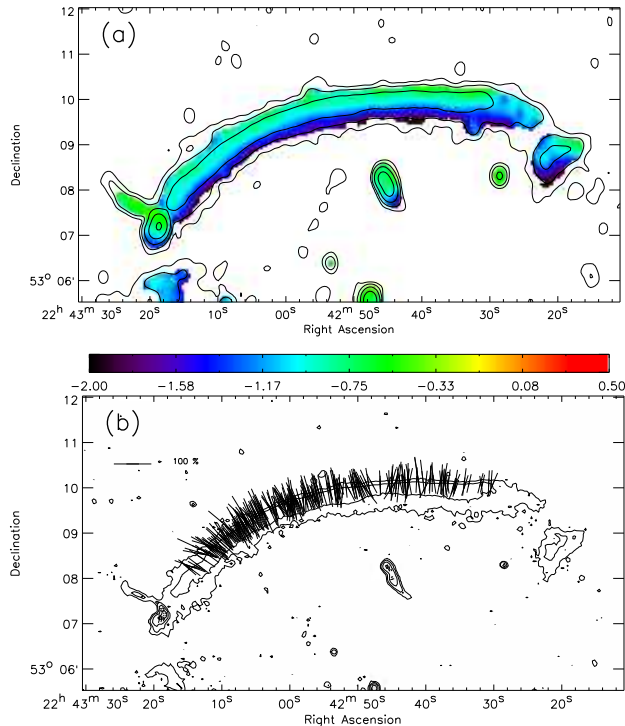


**Fig. 3** Radio spectral index and polarization maps of the relic in CIZA J2242.8+5301. Top: The spectral index was determined using matched observations at 2.3, 1.7, 1.4, 1.2, and 0.61 GHz, fitting a power-law radio spectrum to the flux density measurements. Bottom: The polarization electric field vector map was obtained with the VLA at a frequency of 4.9 GHz. The length of the vectors is proportional the polarization fraction, which is the ratio between the total intensity and total polarized intensity. A reference vector for 100% polarisation is drawn in the top left corner. From van Weeren et al. (2010).

and the line cluster centerradio relic center. The resulting histogram is shown in Fig. 5. From this histogram we see that relics are preferably found along the major axis of the ICM. This is in line with the simple picture that shock waves propagate outwards along the merger axis. We also calculate the angle  $\beta$  between the major axis of the ICM and the relics major axis. Fig. 18 shows that most relics are oriented perpendicular to the ICM major axis, also in agreement with a shock origin for radio relics.

In the next years, simulations should be able to reproduce these trends, and thus constrain the efficiencies of shock acceleration and the magnetic field evolution in clusters. At the same time, it is predicted that *LOFAR* will find of around 100 new radio relics (Hoeft et al. 2008). This will help address some remaining puzzles that surround radio relics, most importantly:

- Which processes accelerate electrons so efficiently at relatively low Mach number ( $M \sim 2 - 4$ ) shocks?

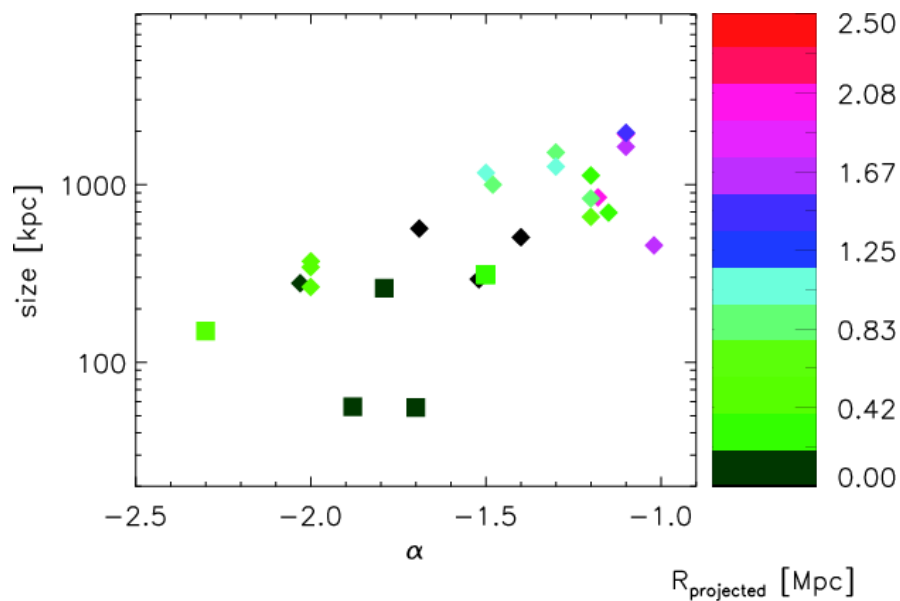


**Fig. 4** Spectral index of radio relics versus their size. Squares are the proposed radio phoenixes. Diamonds represent the radio relics tracing merger shocks where particles are being accelerated by shock acceleration. The color coding is according to the projected distance from the cluster center. For the relics represented by black symbols we could not obtain a reliable projected distance to the cluster center. From van Weeren et al. (2009a).

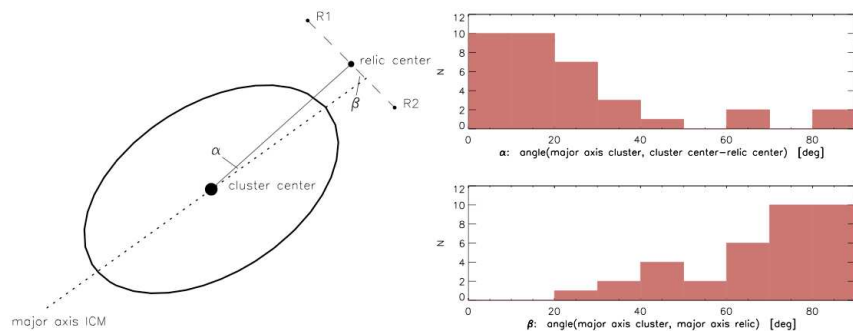


**Fig. 5** Left: Schematic illustration of the angle between the major axis of the ICM and the line relic centercluster center ( $\alpha$ ), and the angle between the relic orientation and major axis of the ICM ( $\beta$ ). Top Right: Histogram of angles between the major axis of the X-ray emission and the line connecting the cluster center with the center of the relic. Bottom Right: Histogram of angles between the major axis of the X-ray emission and the relics major axis. From van Weeren et al. (2011).

- 
- What produces the magnetic fields inside relics? Both the inferred field strengths as well as the observed polarisation of the radio emission need to be explained.
  - Why do some relics have very sharp edges while others appear very fuzzy?
  - Under which conditions do relics form? When do we see single and when double relics?
  - Some relics appear to be connected to cluster-wide radio halo emission. Is there a physical connection between the two?

In the next section, we will review the current state of cosmological simulations that include a treatment for shock acceleration of cosmic rays.

## 5 What we know from simulations

### 5.1 Shocks in cosmological simulations

The statistics of cosmological shocks in the large-scale structure of the Universe has been derived from simulations using, both, Eulerian hydrodynamic codes (e.g. Miniati et al. 2000, 2001, Ryu et al. 2003, Kang et al. 2007, Skillman et al. 2008, Vazza et al. 2010, 2009b,a, Molnar et al. 2009) and smoothed particle hydrodynamic codes (Pfrommer et al. 2007, Hoeft et al. 2008) as well as a number of semi-analytical (Gabici and Blasi 2003, Keshet et al. 2003) studies.

Ryu et al. (2003) performed uniform grid simulations with limited resolution, in which cluster core regions were not properly resolved, while surrounding outskirts were fairly well reproduced (see Fig. 6). Hence, the shocks identified in these simulations are mostly those in cluster outskirts. A cell is determined to have a shock if it meets the following requirements: 1.  $\nabla \cdot \mathbf{v} < 0$ , 2.  $\nabla T \cdot \nabla s > 0$ , 3.  $T_2 > T_1$  and 4.  $\rho_2 > \rho_1$ . where  $\mathbf{v}$  is the velocity field,  $T$  is the temperature,  $\rho$  is the density, and  $s = T/\rho^{\gamma-1}$  is, in X-ray astronomy parlance, the entropy. The subscripts 1 and 2 denote up- and downstream quantities, respectively. To find shocks, one loops through rows of cells along each of the coordinate axes and identifies one-dimensional shock structures in each direction. Fig. 7 shows the surface area,  $S$ , of identified shocks with the preshock gas temperature  $T_1 > 10^7$  K, normalized by the entire volume of the simulation box, at the present epoch as a function of shock Mach number. The quantity  $S$  provides a measure of shock frequency. The Mach number of shocks expected to be found in cluster outskirts is low with  $M \lesssim 3$ . The frequency increases to weakest possible shocks with  $M \sim 1$ .

Vazza et al. (2009b) identifies shocks in cosmological simulations using a method based on velocities (instead of temperatures). They found that the overall differential distribution of shocks with their Mach number in the cosmic volume is very steep, with  $\beta \sim -1.6$  (with  $MdN/dM \propto M^\beta$ ), and the bulk of the detected shocks at any Mach number is found in low-density regions. The Mach number distribution of detected shocks becomes increasingly steeper with ambient density:  $\beta \sim -3$  to  $-4$  is found in clusters and their outskirts. They find that before the epoch of re-ionization,  $z >$

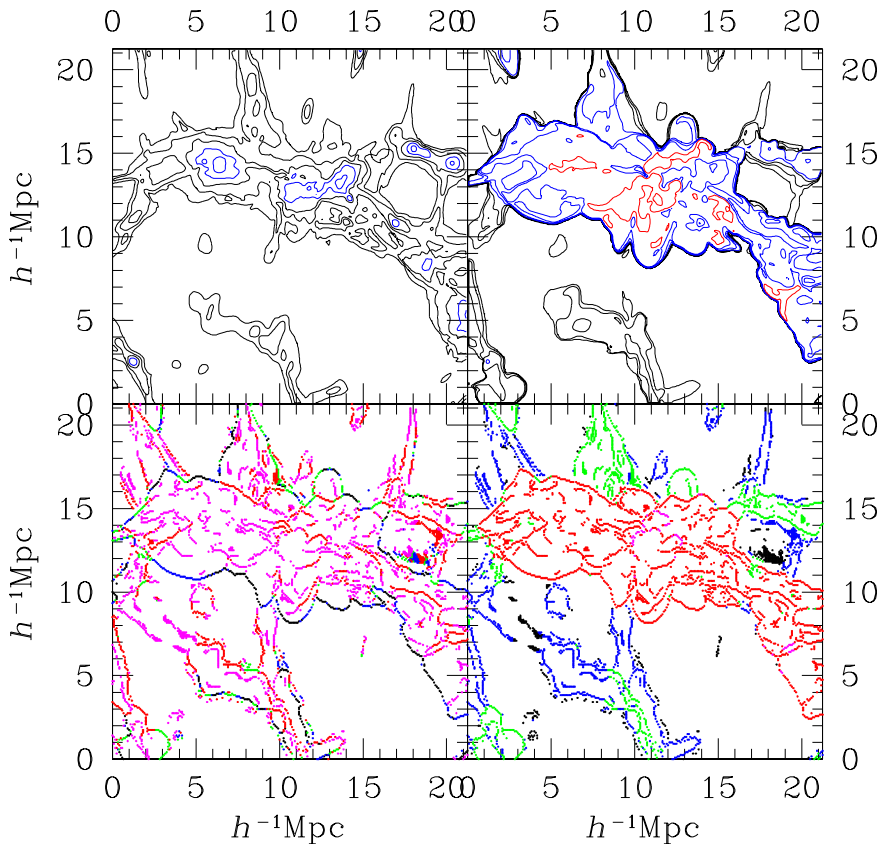


**Fig. 6** Two-dimensional slice around a region containing two clusters/groups at  $z = 0$ . Top panels show the distribution of gas density (left) and temperature (right). Bottom panels show the locations of the shocks, which are color-coded according to shock Mach number  $M$  (left) or shock speed  $v_s$  (right). In the left panel, the colors are coded as follows: black for  $M > 100$ , blue for  $30 < M < 100$ , green for  $10 < M < 30$ , red for  $3 < M < 10$ , and magenta for  $M < 3$ . In the right panel, the colors are coded as follows: black for  $v_s < 15 \text{ km s}^{-1}$ , blue for  $15 < v_s < 65 \text{ km s}^{-1}$ , green for  $65 < v_s < 250 \text{ km s}^{-1}$ , red for  $250 < v_s < 1000 \text{ km s}^{-1}$ , and magenta for  $v_s < 1000 \text{ km s}^{-1}$ .

6, roughly 30 % of the simulated volume is shocked. Then as soon as reionization plays a role, the temperature of the simulated volume increases and the Mach number distribution of shocks at redshift  $z \sim 3 - 6$  undergoes a dramatic change becoming very steep and dominated by weak shocks. The bulk of the energy in their simulations is dissipated in galaxy clusters which contribute about 75 % of the total energy dissipation (about 80 % if the

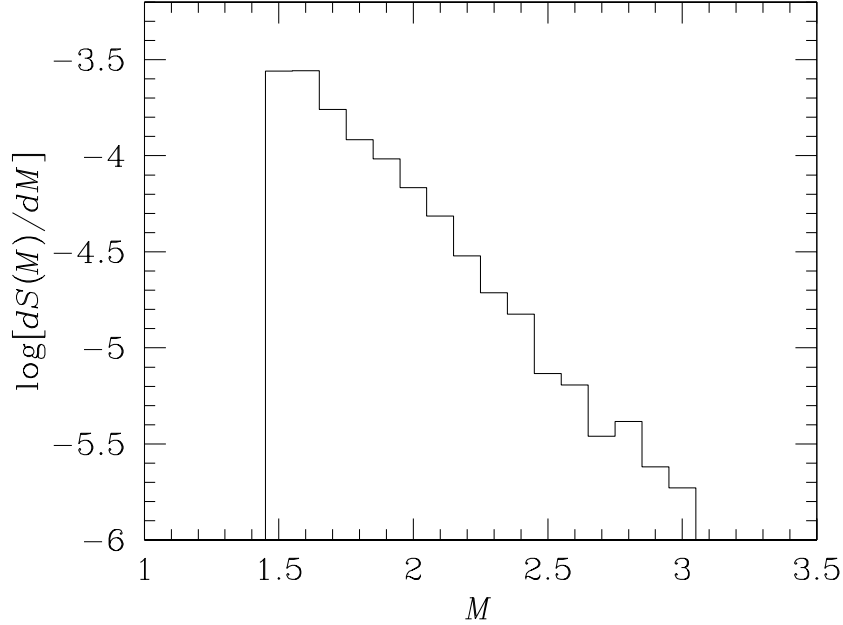


**Fig. 7** Frequency of shocks expected to be found at  $z = 0$  in cluster outskirts as a function of  $M$ . Figure from D. Ryu.

contribution from cluster outskirts is included), while filaments contribute about 15 % of the total energy dissipation.

In line with previous numerical studies, relatively weak shocks are found to dominate the process of energy dissipation in the simulated cosmic volume, although they find a larger ratio between weak and strong shocks with respect to previous studies. The bulk of energy is dissipated at shocks with Mach number  $M \sim 2$  and the fraction of strong shocks decreases with increasing density of the cosmic environments.

Skillman et al. (2008) improved the method employed by Ryu et al. (2003) that can produce errors when examining shocks whose direction of motion is not oriented along a coordinate axis. They find that the Mach number evolution can be interpreted as a method to visualize large-scale structure formation. Shocks with  $M < 5$  typically trace mergers and complex flows, while  $5 < M < 20$  and  $M > 20$  generally follow accretion onto filaments and galaxy clusters, respectively.



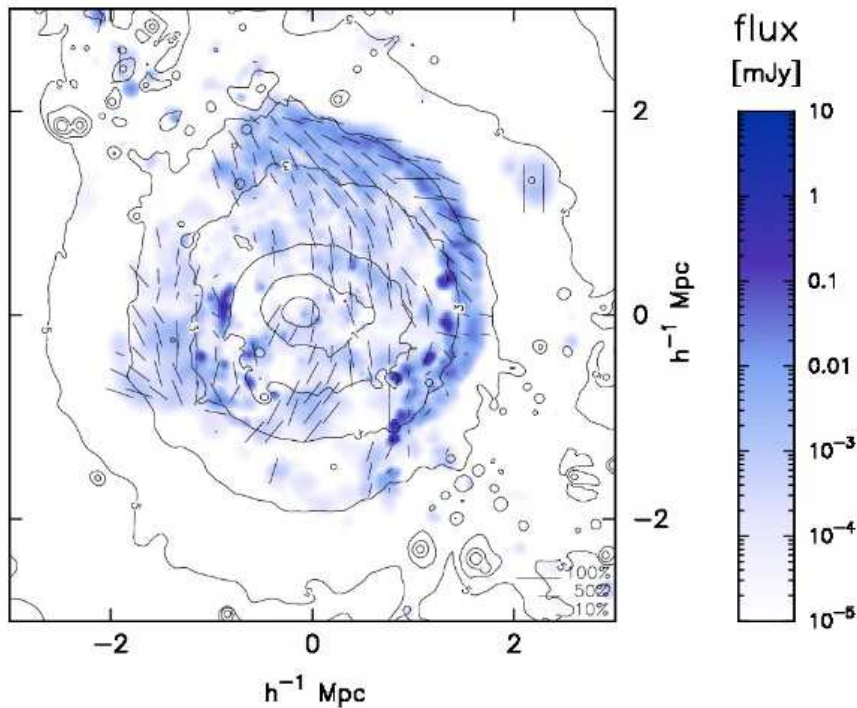


**Fig. 8** Radio emission from a galaxy cluster taken from the Mare Nostrum simulation and resimulated at higher resolution. The vectors denote the degree and the direction of polarisation of the radio emission. The contours indicate the X-ray emission. (From M. Hoeft)

## 5.2 Cosmological simulations with particle acceleration

In recent years a number of cosmological simulations have started to include some treatment of cosmic ray physics with particle acceleration at shocks.

Using a shock-finding formalism tuned to smoothed-particle hydrodynamics simulations, Hoeft et al. (2008) have analyzed the MareNostrum Universe simulation which has  $2 \times 1024^3$  particles in a  $500 h^{-1}$  Mpc box. In addition, they have used the formalism derived in Hoeft and Brüggén (2007) to produce artificial radio maps of massive clusters. Several clusters were found to show radio objects with similar morphologies to observed large-scale radio relics (see Fig. 8), whereas about half of the clusters show only very little radio emission. In agreement with observational findings, the maximum diffuse radio emission of galaxy clusters depends strongly on their X-ray temperature. Moreover, it was found that the so-called accretion shocks cause only very little radio emission.

Using a particle-mesh and Eulerian hydrodynamics code, Ryu et al. have been studying the gas thermalization and CR acceleration efficiencies of shocks in cosmological grid simulations. In order to quantify the energy dissipation at cosmological shocks, the incident shock kinetic energy flux,

$F_{\text{kin}} = (1/2)\rho_1 v_s^3$  where  $\rho_1$  is the preshock gas density, and  $v_s$  the shock velocity, was calculated for each shock, and the results are shown in Fig. 7.

Then, the kinetic energy flux through shock surfaces, normalized by the entire volume of the simulation box, as a function of shock Mach number was calculated. The resulting kinetic energy flux is shown by the dotted line in Fig. 9. The kinetic energy flux through shock surfaces is larger for weaker shocks; energetically weaker shocks are more important processing more shock energy. The acceleration efficiency for cosmic rays,  $\eta$ , depends on the Mach number and the injection parameter,  $\epsilon_B$ , which is defined as  $\epsilon_B \equiv B_0/B_\perp$ , the ratio of the mean magnetic field strength aligned with the shock normal to the amplitude of the postshock turbulent wave field. In addition, it is assumed that the CR population is isotropized with respect to the local Alfvénic wave turbulence, which would in general drift upstream at the Alfvén speed with respect to the bulk plasma. This reduces the velocity difference between upstream and downstream scattering centers compared to the bulk flow, leading to less efficient shock acceleration. Moreover, the dissipation of Alfvén turbulence heats the inflowing plasma in the precursor, which leads to weakening of the subshock strength. (See Kang and Jones (2007) for further discussions and references.)

Fig. 10 shows the gas thermalization and CR acceleration efficiencies, defined as  $\delta(M) \equiv F_{\text{th}}/F_{\text{kin}}$  and  $\eta(M) \equiv F_{\text{CR}}/F_{\text{kin}}$ , respectively, where  $F_{\text{th}}$  and  $F_{\text{CR}}$  are the gas thermal and CR energy flux, respectively, generated at shocks; they are from numerical simulations of quasi-parallel shocks with speed  $v_s = M \cdot 150 \text{ km s}^{-1}$  ( $T_1 = 10^6 \text{ K}$ ), and based on a shock acceleration model of Kang and Jones (2007) with  $\epsilon_B = 0.25$ . At strong shocks with  $M \gtrsim 10$ , the injection rate is high enough so that the CR acceleration efficiency nearly saturates and becomes almost independent of the parameter  $\epsilon_B$ . At weak shocks, on the other hand, the level of injection lies in the regime where the CR acceleration efficiency increases with the injection rate; consequently,  $\eta$  depends sensitively on  $\epsilon_B$ . Note that the value of  $\eta$  presented here is  $\sim 1/2$  of that presented in Kang et al. (2007) for  $M \lesssim 5$ , while it remains about the same for stronger shocks.

By adopting the efficiencies in Fig. 10, the gas thermal and CR energy fluxes dissipated at cosmological shocks as a function of shock Mach number were calculated in the same way the kinetic energy flux through shock surfaces was calculated. The resulting thermal and CR energy fluxes are shown with dashed and solid lines in Fig. 9. For the generation of thermal energy, still weaker shocks are more important; shocks with  $M \lesssim 2.5$  contribute the most to the thermal energy. On the other hand, the generation of CR energy is more efficient at shocks with  $M \gtrsim 2$ . These indicate that in cluster outskirts, while shocks with  $M \lesssim 2$  are more abundant, shocks with  $M \gtrsim 2$  would be more frequently detected as radio relics. We note that the results in Fig. 9 are consistent with those estimated for cosmological shocks in all the regions of the IGM; while shocks around  $M \sim 2$  contribute most to the generation of gas thermal energy, shocks around  $M \sim 3$  contribute most to the generation of CR energy (Ryu et al. 2003, Kang et al. 2007).

At weak shocks, DSA is known to be rather inefficient and the CR pressure remains dynamically insignificant, partly because the injection from thermal

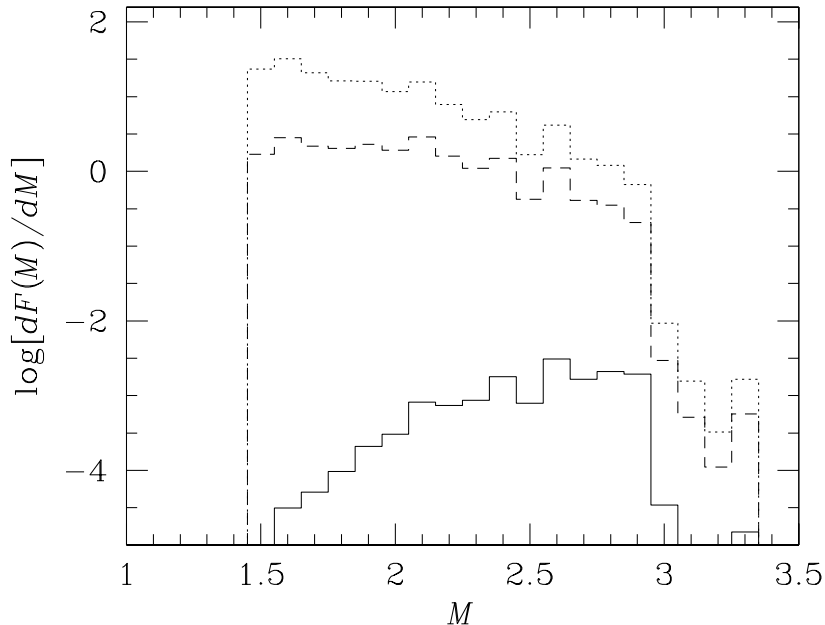


**Fig. 9** Dotted line: Kinetic energy flux per comoving volume passing through surfaces of shocks in cluster outskirts as a function of  $M$  at  $z = 0$ . Dashed line: Gas thermal energy dissipated at the shocks as a function of  $M$ . Solid line: CR energy accelerated at the shocks as a function of  $M$ . All the quantities are in units of  $10^{40} \text{ ergs s}^{-1} (h^{-1} \text{ Mpc})^{-3}$

to nonthermal particles is inefficient (e.g., Kang et al. 2002). Recently, Kang & Ryu (2010) found that at weak shocks expected to form in clusters much less than  $10^{-3}$  of particles are injected into CRs and much less than  $\sim 1\%$  of the shock ram pressure is converted into the downstream pressure of CR protons, so the particle acceleration is virtually negligible.

This has been followed up in recent AMR simulations by Vazza (2011 in prep.) that implement prescriptions for CR acceleration at shocks. This work suggests that the shock acceleration efficiency needs to be increased in order to explain the occurrence of radio relics. Kang et al. (2007) have already suggested that pre-existing populations of cosmic rays can boost the acceleration efficiency significantly, and this may be part of the answer. Thus

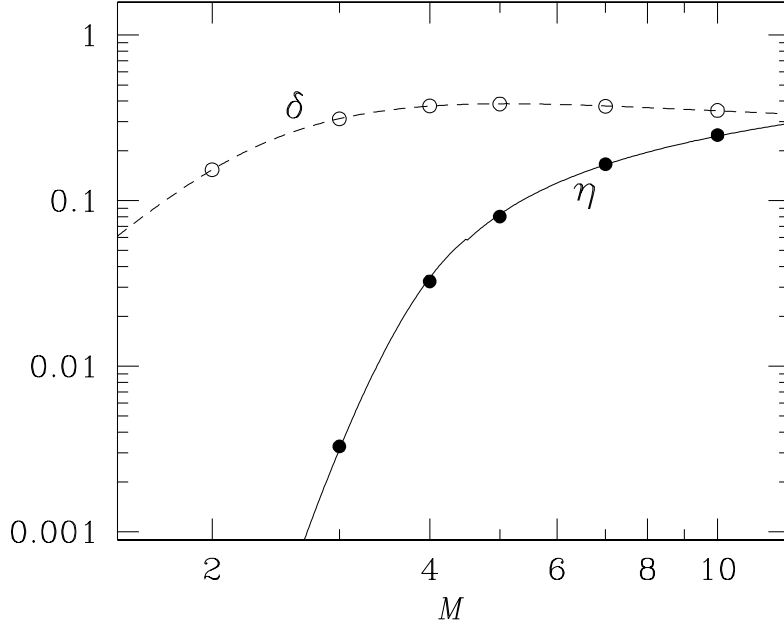


**Fig. 10** Gas thermalization efficiency,  $\delta(M)$ , and CR acceleration efficiency,  $\eta(M)$ , as a function of Mach number. Open and filled circles are the values estimated from numerical simulations based on a shock acceleration model and dashed and solid lines are the fits.

the observations of cluster radio relics can inform us about the microphysics in weak shocks. This will be the subject of the next section.

## 6 Microphysics of shocks

### 6.1 Plasma physics in CR-modified shocks

The heating processes in collisionless shocks are complex phenomena. The *irreversible* transformation of a part of the kinetic energy of the ordered bulk motion of the upstream flow into the energy of the random motions of plasma particles in the downstream flow in collisionless shocks is due to the plasma instabilities in the thin dissipation region where the wave-particle

interactions provide momentum and energy redistribution between different components.

The front of a strong collisionless shock wave may consist of a precursor and a viscous velocity discontinuity (subshock) of a local Mach number that is smaller than the total Mach number of the shock wave (Fig. 11). The compression of matter at the subshock can be much lower than the total compression of the medium in the shock wave allowing for a high compression in the precursor. We refer to such shocks as CR-modified. The standard collisional model of a strong single-fluid shock predicts a particle temperature  $kT \rightarrow (3/16) \cdot m v_{\text{sh}}^2$  for  $\gamma_g = 5/3$ . However, this is not generally valid in multi-fluid plasma and CR-modified shocks since the total shock compression ratio,  $R_t(v_{\text{sh}})$ , depends on the shock velocity,  $v_{\text{sh}}$ , in the strong shock limit.

In a simplified steady-state model, a strong CR-modified shock can be parameterized by the total Mach number of the shock  $\mathcal{M}_{\text{tot}}$  and the Mach number of the subshock  $\mathcal{M}_{\text{sub}}$ . Then the downstream ion temperature  $T_i^{(2)}$  can be estimated for the CR modified shock of a given velocity  $v_{\text{sh}}$  if the total compression ratio,  $R_t$ , is known:

$$T_i^{(2)} \approx \phi(\mathcal{M}_{\text{sub}}) \cdot \frac{\mu v_{\text{sh}}^2}{\gamma_g R_t^2(v_{\text{sh}})}, \quad \text{where } \phi(\mathcal{M}_{\text{sub}}) = \frac{2\gamma_g \mathcal{M}_{\text{sub}}^2 - (\gamma_g - 1)}{(\gamma_g - 1)\mathcal{M}_{\text{sub}}^2 + 2}. \quad (2)$$

The total compression ratio  $R_t$  in Eq. 2 depends on the precursor heating rate and it is the main parameter in the steady state CR modified shock to determine the postshock ion temperature  $T_i^{(2)}$  (Bykov 2005, Bykov et al. 2008a).

Shocks may also generate turbulence through cosmic-ray driven instabilities. In the shock precursor, this turbulence is certain to play a critical role in non-linear models of strong, CR-modified shocks. Different non-linear approaches to the modeling of the large-scale structure of a shock undergoing efficient cosmic ray acceleration (e.g., Bell and Lucek 2001, Amato and Blasi 2006, Vladimirov et al. 2006, Bell 2004, Vladimirov et al. 2008, Zirakashvili et al. 2008, Kang et al. 2009) have been proposed. Many of these have predicted the presence of strong MHD turbulence in the shock precursor. An exact modeling of the shock structure in a turbulent medium, including nonthermal particle injection and acceleration, requires a nonperturbative, self-consistent description of a multi-component and multi-scale system including the strong MHD-turbulence dynamics.

A Monte-Carlo model of nonlinear diffusive shock acceleration accounting for magnetic field amplification through resonant instabilities induced by accelerated particles, and including the effects of dissipation of turbulence upstream of a shock and the subsequent precursor plasma heating was studied by Vladimirov et al. (2008). Feedback effects between the plasma heating due to turbulence dissipation and particle injection are strong, adding to the nonlinear nature of efficient shock acceleration.

Describing the turbulence damping in a parametrized way, Vladimirov et al. (2008) reach two important results: first, for conditions typical of supernova remnant shocks, even a small amount of dissipated turbulence energy ( $\sim 10\%$ ) is sufficient to significantly heat the precursor plasma, and second,

the heating upstream of the shock leads to an increase in the injection of thermal particles at the subshock by a factor of a few. In their results, the response of the non-linear shock structure to the boost in particle injection prevented the efficiency of particle acceleration and magnetic field amplification from increasing. The non-linear models with turbulence generation and dissipation may lead to a scenario in which particle injection boost due to turbulence dissipation results in more efficient acceleration and even stronger amplified magnetic fields than without dissipation. In Fig. 11 the effects are illustrated for a stationary, non-linear Monte-Carlo simulation of a forward shock in a supernova remnant of velocity of  $5,000 \text{ km s}^{-1}$  accelerating particles up to maximal energies of about  $10^5 \text{ GeV}$  (Vladimirov et al. 2008). The shock velocity is higher than is expected for cluster accretion shocks but the simulation can be used to investigate the qualitative behavior and to obtain the appropriate scalings. The maximal energy depends on the ratio of the shock scale size and particle escape physics that is simply modeled by a free escape boundary in the Monte Carlo simulation. Ultra-high energy CR acceleration above  $10^9 \text{ GeV}$  by cluster accretion shocks was shown by Norman et al. (1995) and Kang et al. (1996) to be a plausible scenario. In that case the scale size of CR precursor with magnetic field amplification can be about 100 kpc.

Vladimirov et al. (2008) demonstrated that the effect of turbulent dissipation on the thermal plasma is evident in the values of the pre-subshock temperature  $T_1$ , the downstream temperature  $T_2$ , and the volume-averaged precursor temperature  $\langle T(x < 0) \rangle$  (the averaging takes place over the CR precursor region). The temperatures were calculated from the thermal particle pressure using the ideal gas law. The value of the pre-subshock temperature  $T_1$  depends drastically on the level of the turbulent dissipation  $\alpha_H$ , increasing from  $\alpha_H = 0$  to  $\alpha_H = 0.5$  by a factor of 11 in the case of  $T = 10^6 \text{ K}$ . It is less in the case of  $T = 10^6 \text{ K}$  than for  $T \sim 10^4 \text{ K}$  because the efficiency of the CR streaming instability in generating the magnetic turbulence is less for the smaller Mach number. The values of the temperature as high as  $T_1$  are achieved upstream only near the subshock; the volume-averaged upstream temperature,  $\langle T(x < 0) \rangle$ , is significantly lower. The factor by which the average temperature  $\langle T(x < 0) \rangle$  increases in case of  $T \sim 10^6 \text{ K}$  is about 2.3. The multi-fluid processes described above can preheat the accreting gas. An important prediction of the models of strong shocks is the possibility to amplify an initial seed magnetic field by a few orders of magnitude. CR currents and CR pressure gradients upstream of the strong shock can drive magnetic fluctuations on the shock precursor scale length. The precursor scale size is  $10^9$  times larger than the subshock transition region where strong, small-scale magnetic field fluctuations are directly produced by instabilities of super-Alfvénic bulk plasma flows. These small-scale fluctuations are responsible for bulk dissipation and the adiabatic amplification of the transverse magnetic field in collisionless shocks. From Fig. 11, it is clear that the magnetic field amplification factor depends on the non-linear processes of particle injection through turbulent dissipation in the shock precursor.

Above, we discussed the ion temperature in multi-fluid shocks. However, cluster X-ray spectra depend primarily on the electron temperature, while

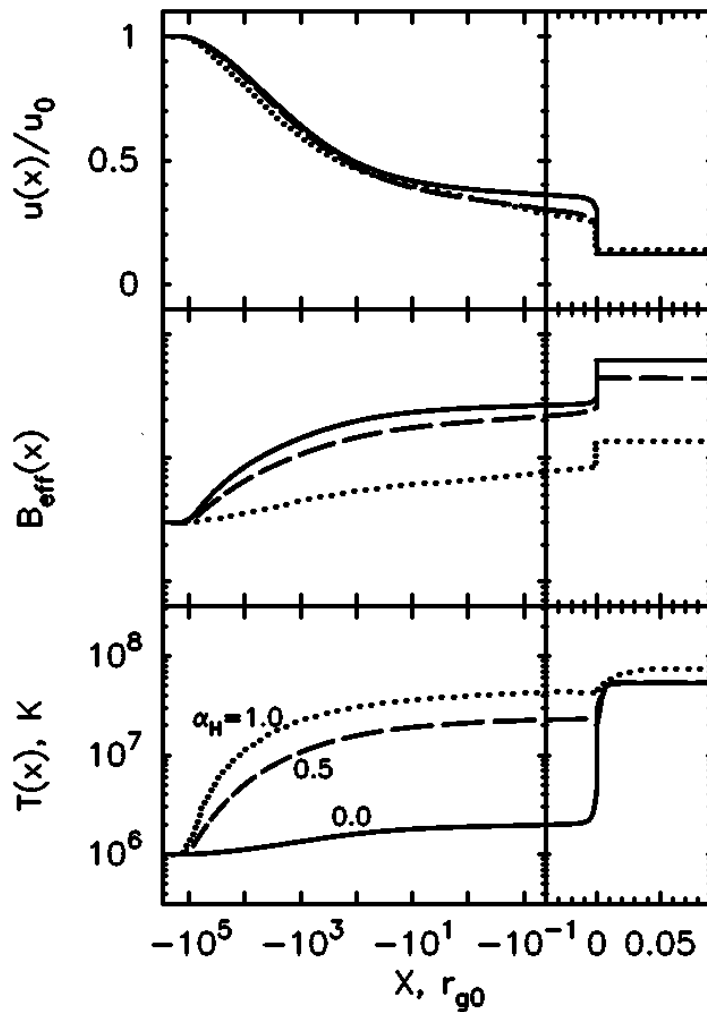


**Fig. 11** Results of non-linear simulations in the case of the far upstream temperature  $T = 10^6$  K with different values of turbulence dissipation parameter  $\alpha_H$  taken from Vladimirov et al. (2008). The solid, dashed and dotted lines correspond, respectively, to  $\alpha_H = 0, 0.5$  and  $1.0$ . The plotted quantities are the bulk flow speed  $u(x)$ , the effective amplified magnetic field  $B_{\text{eff}}(x)$  and the thermal gas temperature  $T(x)$ . The shock is located at  $x = 0$ . There is a change from the logarithmic to the linear scale at  $x = -0.05$ . The distances are measured in relativistic proton gyroradius unit  $r_{g0}$ .

MHD-type wave dissipation in the shock precursor may preferentially heat ions. However, the complete  $e - i$  Coulomb equilibration requires the system age  $\tau_{ei} \gtrsim 10^{10} T_6^{3/2}/n$ , where the postshock density  $n$  is measured in  $\text{cm}^{-3}$ , the ion temperature  $T_6$  is in  $10^6$  K, and  $\tau_{ei}$  is in seconds Mewe (1990). Since the number density around the cluster virial radius is typically above  $10^{-5}$ ,  $\text{cm}^{-3}$ , the temperature equilibration scale length in the accretion shock

precursor is below 100 kpc. The electron temperature downstream of the shock depends on collisionless electron heating e.g. (Bykov and Uvarov 1999, Rakowski et al. 2008, Bykov et al. 2008b). Non-resonant interactions of the electrons with strong nonlinear fluctuations generated by kinetic instabilities of the ions in the transition region inside the shock front may play the main role in the heating and pre-acceleration of the electrons, as it was shown in the model by Bykov and Uvarov (1999). They calculated the electron energy spectrum in the vicinity of shock waves and showed that the heating and pre-acceleration of the electrons occur on a scale of the order of several hundred ion inertial lengths  $l_i$  in the vicinity of a viscous discontinuity. Although the electron distribution function is significantly out of equilibrium near the shock front, its low energy part can be approximated by a Maxwellian distribution.

The effect of the non-adiabatic electron heating efficiency,  $\beta_e$ , on the degree of non-equipartition was studied recently by Wong and Sarazin (2009). They have shown that for a cluster with a mass of  $M_{\text{vir}} \sim 1.2 \times 10^{15} M_{\odot}$ , electron and ion temperatures differ by less than a percent within the virial radius. The difference is 20% for a non-adiabatic electron heating efficiency of 1/1800 to 0.5 at  $\sim 1.4$  of the virial radius. Beyond this radius, the non-equipartition effect depends rather strongly on  $\beta_e$  (Wong and Sarazin 2009), and such a strong dependence at the shock radius can be used to distinguish shock heating models or constrain the shock heating efficiency of electrons.

As opposed to semi-analytic kinetic theory methods (Achterberg et al. 2001, Keshet and Waxman 2005) or Monte Carlo test-particle simulations (Niemić and Ostrowski 2004, Ellison and Double 2004), PIC simulations can tackle the problem of particle acceleration in shocks without the need for simplifying assumptions about the nature of the magnetic turbulence or the details of wave-particle interactions. Multi-dimensional PIC simulations of relativistic un-magnetized shocks have been presented, e.g. by Spitkovsky (2008) for electron-ion flows. Kato and Takabe (2010) present a two-dimensional particle-in-cell simulation to investigate weakly magnetized perpendicular shocks. The simulated thermal energies of electrons and ions in the downstream region are not in equipartition but their temperature ratio  $\beta_e = T_e/T_i \sim 0.3 - 0.4$  is high enough indicating rather efficient non-adiabatic heating of the electrons in the shock transition region.

Using 2.5D PIC simulations, Sironi and Spitkovsky (2010) find that in subluminal shocks, where relativistic particles can escape ahead of the shock along the magnetic field lines, ions are efficiently accelerated via a Fermi-like mechanism. The scattering is provided by short-wavelength non-resonant modes produced by Bell's instability (Bell 2004), whose growth is seeded by the current of shock-accelerated ions that propagate ahead of the shock. Upstream electrons enter the shock with lower energy than ions, so they are more strongly tied to the field. As a result, only about 1% of the incoming electrons are Fermi-accelerated at the shock before they are advected downstream, where they populate a steep power-law tail. Thus, efficient electron heating is the universal property of relativistic electron-ion shocks, but significant nonthermal acceleration of electrons is hard to achieve in magnetized flows and requires weakly magnetized shocks, where magnetic fields



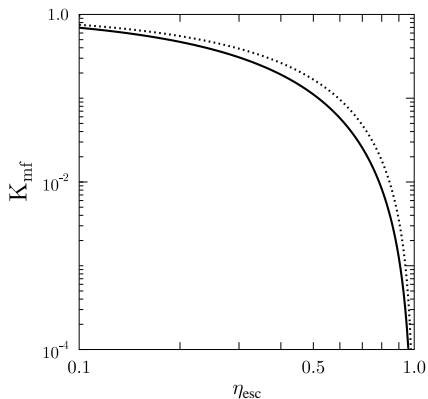


**Fig. 12** Normalized post-shock gas entropy,  $K_{\text{mf}} = K_0 T / \rho^{(\gamma_g - 1)}$ , as a function of the CR particle energy escape flux  $Q_{\text{esc}}$  carried by energetic particles. The dimensionless flux is defined as  $\eta_{\text{esc}} = Q_{\text{esc}} / \Pi_{\text{kin}}$ , where  $\Pi_{\text{kin}} = \rho_1 v_{\text{sh}}^3 / 2$ . The upper curve (dotted) corresponds to an effective adiabatic exponent  $\gamma_g = 4/3$  (relativistic gas), while the lower (solid) curve corresponds to  $\gamma_g = 5/3$ . The postshock entropy is normalized to  $K_{\text{mf}}(\eta_{\text{esc}} = 0)$ .

self-generated via the Weibel instability are stronger than the background field.

## 6.2 Entropy in CR-modified Accretion Shocks

A distinctive feature of CR-modified shocks is their high gas compression factor  $R_t(v_{\text{sh}})$  that can be much higher than the single fluid shock limit of  $(\gamma_g + 1) / (\gamma_g - 1)$ . Since the postshock gas entropy for a strong multi-fluid shock scales as  $R_t(v_{\text{sh}})^{-(\gamma_g + 1)}$ , it can be significantly reduced compared to the single-fluid adiabatic shock of the same velocity (*e.g.*, Bykov et al. 2008a). The effects are due to energetic particle acceleration and magnetic field generation. Energetic particles can penetrate into the shock upstream region. They are coupled with the upstream gas through fluctuating magnetic fields (including the Alfvén waves). Magnetic field dissipation provides gas pre-heating and entropy production in the shock precursor. Energetic particles deplete the momentum distribution in the gas resulting in a higher gas compression and a reduced temperature. In Fig. 12 the post-shock gas entropy is shown as a function of the fraction  $\eta_{\text{esc}}$ . The curves were calculated for a strong shock with no precursor heating *i.e.*  $\alpha_H = 0$ .

In galaxy clusters, entropy profiles have been measured by Pratt et al. (2010) at least out to  $R_{1000}$  in 31 nearby galaxy clusters from the *XMM-Newton* cluster structure survey (REXCESS) and out to  $R_{500}$  in thirteen systems. The effects of CRs on the entropy production in shocks illustrated above can be of importance for accretion shocks that are expected to be located at larger radii. It will require deeper exposures of the next generation

telescopes to measure the entropy profiles at these radii. The entropy in the inner cluster regions can be also affected by internal shocks if the shocks are efficient accelerators of CRs. The current entropy profile simulations (e.g. Borgani et al. 2008, Borgani and Kravtsov 2009) ought to be extended to include CR physics.

## 7 Summary

It is only now, with low-frequency radio telescopes, long exposures with high-resolution X-ray satellites and  $\gamma$ -ray telescopes, that we are beginning to learn about the physics of cluster outskirts. In the coming years SZ telescopes are going to deliver further insights into the plasma physics of these special regions in the Universe. The last years have already shown tremendous progress with detections of shocks, estimates of magnetic field strengths and constraints on the particle acceleration efficiency. The main points of this review are listed below:

- Cosmological shocks are collisionless: Coulomb collisions are not sufficient to provide the viscous dissipation of the incoming flow, and collective effects play a major role.
- Collisionless shocks generate energetic, non-thermal particles that can penetrate far into the upstream flow. The particles decelerate the flow and preheat the gas. They can also efficiently generate strong fluctuating magnetic fields in the upstream region. This turbulence, which may result from cosmic-ray driven instabilities, in the shock precursor, is certain to play a critical role in non-linear models of strong, CR-modified shocks.
- A few merger shocks have been identified in X-rays, exhibiting both a sharp gas density edge and an unambiguous temperature jump: in the "bullet cluster", 1E 065756 (Markevitch et al. 2002), A520 (Markevitch et al. 2005) and Abell 2146 (Russell et al. 2010).
- On the basis of X-ray observations, microphysical properties of shocks can be derived. Markevitch et al. (2006) find that the temperatures across merger shocks are consistent with instant heating; equilibration between electrons and protons on the collisional timescale is excluded. The electron temperature downstream of the shock depends on collisionless electron heating e.g. (Bykov and Uvarov 1999, Rakowski et al. 2008, Bykov et al. 2008b). Non-resonant interactions of the electrons with strong nonlinear fluctuations generated by kinetic instabilities of the ions in the transition region inside the shock front may play the main role in the heating and pre-acceleration of the electrons. Future X-ray observations extending to the virial radius or even close to the shock radius should be able to detect signatures of non-equipartition at shocks.
- *Suzaku* observations provide evidence for departures from hydrostatic equilibrium around and even before the virial radius as it is seen in the galaxy cluster Abell 1795 (e.g., Bautz et al. 2009). Evidence for nonthermal pressure support suggests that bulk motions from mergers could be making a significant contribution to the gas energy in the outskirts of this cluster (George et al. 2009).

- 
- Recently discovered radio relics provide very strong evidence for shock acceleration at merger shock waves in galaxy clusters. Van Weeren et al. (2010) find that on average smaller radio relics have steeper spectra. Such a trend is in line with predictions from shock statistics derived from cosmological simulations (Skillman et al. 2008, Battaglia et al. 2009, Hoeft et al. 2008). They find that larger shock waves occur mainly in lower-density regions and have larger Mach numbers, and consequently shallower spectra.
  - Observations of radio relics in combination with X-ray observations suggest magnetic field strengths in relics of  $> 3 \mu\text{G}$  and efficiencies of 0.2% of the kinetic energy dissipated in a shock going into relativistic electrons (Finoguenov et al. 2009, van Weeren et al. 2010) .
  - Radio relics also suggest that the efficiency of shock acceleration at weak shocks is higher than predicted in theories of diffusive shock acceleration.
  - The bulk of the energy in their simulations is dissipated in galaxy clusters which contribute about 75 % of the total energy dissipation (about 80 % the contribution from cluster outskirts is included), while filaments contribute about 15 % of the total energy dissipation. In agreement with observational findings, the maximum diffuse radio emission of galaxy clusters depends strongly on their X-ray temperature. While shocks around  $M \sim 2$  contribute most to the generation of gas thermal energy, shocks around  $M \sim 3$  contribute most to the generation of CR energy (Ryu et al. 2003, Kang et al. 2007).
  - The effects of CRs on entropy production in shocks as illustrated above can be of importance for accretion shocks that are expected to be located at larger radii. It will require deeper exposures of the next generation telescopes to measure the entropy profiles at these radii.

Many open questions remain. So far still little is known about shock acceleration and magnetic field generation in clusters, nor about the microstructure of shocks in very dilute plasmas.

Most likely, all these processes are related and their understanding requires input from, both, observations and theory. The next years will see a rapid growth in observational data. On the theoretical side, we expect substantial progress from new techniques that simulate particle acceleration in a magnetohydrodynamical setting. Fully kinetic particle-in-cell simulations provide a powerful tool for exploration of the structure of collisionless shocks from first principles, thus determining self-consistently the interplay between shock-generated waves and accelerated particles (Sironi and Spitkovsky 2010). Results from these simulations can then serve as input for cosmological simulations that include CR-physics.

**Acknowledgements** We thank an anonymous referee for a very careful read of our manuscript. MB acknowledges support by the DFG Research Unit "Magnetisation of Interstellar and Intergalactic Media: The Prospects of Low-Frequency Radio Observations". DR was supported in part by R&D Program through the National Fusion Research Institute of Korea funded by the Government funds. A.M.B. was supported in part by RBRF grants 09-02-12080, 11-02-00429a, by the RAS Presidium Programm, and the Russian government grant 11.G34.31.0001 to Sankt-Petersburg State Politechnical University. He performed some of the simulations at

the Joint Supercomputing Centre (JSCC RAS) and the Supercomputing Centre at Ioffe Institute, St.Petersburg. We thank Aurora Simionescu, Matthias Hoeft and Franco Vazza for helpful comments on the manuscript. Finally, the authors would like the convenors of the workshop in Bern for their initiative and excellent work and the staff at ISSI for their support.

## References

- A. Achterberg, Y.A. Gallant, J.G. Kirk, A.W. Guthmann, Particle acceleration by ultrarelativistic shocks: theory and simulations. *Mon. Not. Royal Astron. Soc.* **328**, 393–408 (2001). doi:10.1046/j.1365-8711.2001.04851.x
- M. Ackermann, M. Ajello, A. Allafort, L. Baldini, J. Ballet, G. Barbiellini, D. Bastieri, K. Bechtol, R. Bellazzini, R.D. Blandford, P. Blasi, E.D. Bloom, E. Bonamente, GeV Gamma-ray Flux Upper Limits from Clusters of Galaxies. *Astrophys. J. Lett.* **717**, 71–78 (2010). doi:10.1088/2041-8205/717/1/L71
- F. Aharonian, A.G. Akhperjanian, G. Anton, U. Barres de Almeida, A.R. Bazer-Bachi, Y. Becherini, B. Behera, K. Bernlöhr, C. Boisson, A. Bochow, V. Borrel, E. Brion, J. Brucker, P. Brun, R. Bühler, T. Bulik, I. Büsching, T. Bouteiller, P.M. Chadwick, A. Charbonnier, R.C.G. Chaves, A. Cheesebrough, Constraints on the multi-TeV particle population in the Coma galaxy cluster with HESS observations. *Astron. Astrophys.* **502**, 437–443 (2009). doi:10.1051/0004-6361/200912086
- M. Ajello, P. Rebusco, N. Cappelluti, O. Reimer, H. Böhringer, J. Greiner, N. Gehrels, J. Tueller, A. Moretti, Galaxy Clusters in the Swift/Burst Alert Telescope Era: Hard X-rays in the Intracluster Medium. *Astrophys. J.* **690**, 367–388 (2009). doi:10.1088/0004-637X/690/1/367
- E. Amato, P. Blasi, Non-linear particle acceleration at non-relativistic shock waves in the presence of self-generated turbulence. *Mon. Not. Royal Astron. Soc.* **371**, 1251–1258 (2006). doi:10.1111/j.1365-2966.2006.10739.x
- W.I. Axford, E. Leer, G. Skadron, The Acceleration of Cosmic Rays by Shock Waves, in *International Cosmic Ray Conference*. International Cosmic Ray Conference, vol. 11, 1977, p. 132
- J. Bagchi, F. Durret, G.B.L. Neto, S. Paul, Giant Ringlike Radio Structures Around Galaxy Cluster Abell 3376. *Science* **314**, 791–794 (2006). doi:10.1126/science.1131189
- N. Battaglia, C. Pfrommer, J.L. Sievers, J.R. Bond, T.A. Enßlin, Exploring the magnetized cosmic web through low-frequency radio emission. *Mon. Not. Royal Astron. Soc.* **393**, 1073–1089 (2009). doi:10.1111/j.1365-2966.2008.14136.x
- M.W. Bautz, E.D. Miller, J.S. Sanders, K.A. Arnaud, R.F. Mushotzky, F.S. Porter, K. Hayashida, J.P. Henry, J.P. Hughes, M. Kawaharada, K. Makashima, M. Sato, T. Tamura, Suzaku Observations of Abell 1795: Cluster Emission to  $r_{200}$ . *PASJ* **61**, 1117 (2009)
- A.R. Bell, The acceleration of cosmic rays in shock fronts. I. *Mon. Not. Royal Astron. Soc.* **182**, 147–156 (1978a)
- A.R. Bell, The acceleration of cosmic rays in shock fronts. II. *Mon. Not. Royal Astron. Soc.* **182**, 443–455 (1978b)
- A.R. Bell, Turbulent amplification of magnetic field and diffusive shock acceleration of cosmic rays. *Mon. Not. Royal Astron. Soc.* **353**, 550–558 (2004). doi:10.1111/j.1365-2966.2004.08097.x
- A.R. Bell, S.G. Lucek, Cosmic ray acceleration to very high energy through the non-linear amplification by cosmic rays of the seed magnetic field. *Mon. Not. Royal Astron. Soc.* **321**, 433–438 (2001). doi:10.1046/j.1365-8711.2001.04063.x
- E. Belsole, J. Sauvageot, G.W. Pratt, H. Bourdin, Merging clusters of galaxies observed with XMM-Newton. *Advances in Space Research* **36**, 630–635 (2005). doi:10.1016/j.asr.2005.01.029
- E.W. Bertschinger, Nonlinear growth of perturbations in an Einstein-De Sitter cosmology, PhD thesis, Princeton Univ., NJ., 1984

- 
- R. Blandford, D. Eichler, Particle Acceleration at Astrophysical Shocks - a Theory of Cosmic-Ray Origin. *Phys. Rep.* **154**, 1 (1987). doi:10.1016/0370-1573(87)90134-7
- R.D. Blandford, J.P. Ostriker, Particle acceleration by astrophysical shocks. *Astrophys. J. Lett.* **221**, 29–32 (1978). doi:10.1086/182658
- H. Böhringer, N. Werner, X-ray spectroscopy of galaxy clusters: studying astrophysical processes in the largest celestial laboratories. *AAPR* **18**, 127–196 (2010). doi:10.1007/s00159-009-0023-3
- A. Bonafede, G. Giovannini, L. Feretti, F. Govoni, M. Murgia, Double relics in Abell 2345 and Abell 1240. Spectral index and polarization analysis. *Astron. Astrophys.* **494**, 429–442 (2009). doi:10.1051/0004-6361:200810588
- S. Borgani, A. Kravtsov, Cosmological simulations of galaxy clusters. (2009)
- S. Borgani, A. Diaferio, K. Dolag, S. Schindler, Thermodynamical Properties of the ICM from Hydrodynamical Simulations. *Space Science Reviews* **134**, 269–293 (2008). doi:10.1007/s11214-008-9317-4
- M. Brüggen, S. Heinz, E. Roediger, M. Ruszkowski, A. Simionescu, Shock heating by Fanaroff-Riley type I radio sources in galaxy clusters. *Mon. Not. Royal Astron. Soc.* **380**, 67–70 (2007). doi:10.1111/j.1745-3933.2007.00351.x
- G. Brunetti, A. Lazarian, Acceleration of primary and secondary particles in galaxy clusters by compressible MHD turbulence: from radio haloes to gamma-rays. *Mon. Not. Royal Astron. Soc.* **410**, 127–142 (2011). doi:10.1111/j.1365-2966.2010.17457.x
- G. Brunetti, P. Blasi, R. Cassano, S. Gabici, High energy emission from galaxy clusters and particle acceleration due to MHD turbulence, in *American Institute of Physics Conference Series*, ed. by D. Bastieri & R. Rando. American Institute of Physics Conference Series, vol. 1112, 2009, pp. 129–137. doi:10.1063/1.3125773
- A.M. Bykov, Multi-fluid shocks in clusters of galaxies: Entropy,  $\sigma_v T$ ,  $MT$  and  $L_X T$  scalings. *Advances in Space Research* **36**, 738–746 (2005). doi:10.1016/j.asr.2005.01.052
- A.M. Bykov, Y.A. Uvarov, Electron kinetics in collisionless shock waves. *JETP* **88**, 465–475 (1999)
- A.M. Bykov, K. Dolag, F. Durret, Cosmological Shock Waves. *Space Science Reviews* **134**, 119–140 (2008a). doi:10.1007/s11214-008-9312-9
- A.M. Bykov, S.M. Osipov, D.C. Ellison, Cosmic ray current driven turbulence in shocks with efficient particle acceleration: the oblique, long-wavelength mode instability. *Mon. Not. Royal Astron. Soc.* **410**, 39–52 (2011). doi:10.1111/j.1365-2966.2010.17421.x
- A.M. Bykov, F.B.S. Paerels, V. Petrosian, Equilibration Processes in the Warm-Hot Intergalactic Medium. *Space Science Reviews* **134**, 141–153 (2008b). doi:10.1007/s11214-008-9309-4
- A. Cattaneo, S.M. Faber, J. Binney, A. Dekel, J. Kormendy, R. Mushotzky, A. Babul, P.N. Best, M. Brüggen, A.C. Fabian, C.S. Frenk, A. Khalatyan, H. Netzer, A. Mahdavi, J. Silk, M. Steinmetz, L. Wisotzki, The role of black holes in galaxy formation and evolution. *Nature* **460**, 213–219 (2009). doi:10.1038/nature08135
- E. Churazov, W. Forman, C. Jones, R. Sunyaev, H. Böhringer, XMM-Newton observations of the Perseus cluster - II. Evidence for gas motions in the core. *Mon. Not. Royal Astron. Soc.* **347**, 29–35 (2004). doi:10.1111/j.1365-2966.2004.07201.x
- K. Dolag, A.M. Bykov, A. Diaferio, Non-Thermal Processes in Cosmological Simulations. *SSR* **134**, 311–335 (2008). doi:10.1007/s11214-008-9319-2
- L.O. Drury, An introduction to the theory of diffusive shock acceleration of energetic particles in tenuous plasmas. *Reports on Progress in Physics* **46**, 973–1027 (1983). doi:10.1088/0034-4885/46/8/002
- F. Durret, J.S. Kaastra, J. Nevalainen, T. Ohashi, N. Werner, Soft X-Ray and Extreme Ultraviolet Excess Emission from Clusters of Galaxies. *Space Science Reviews* **134**, 51–70 (2008). doi:10.1007/s11214-008-9313-8
- D.C. Ellison, G.P. Double, Diffusive shock acceleration in unmodified relativistic, oblique shocks. *Astroparticle Physics* **22**, 323–338 (2004).

- doi:10.1016/j.astropartphys.2004.08.005
- S. Ettori, S. Molendi, X-ray observations of cluster outskirts: current status and future prospects. ( 2010)
- L. Feretti, H. Böhringer, G. Giovannini, D. Neumann, The radio and X-ray properties of Abell 2255. *Astron. Astrophys.* **317**, 432–440 (1997)
- C. Ferrari, F. Govoni, S. Schindler, A.M. Bykov, Y. Rephaeli, Observations of Extended Radio Emission in Clusters. *Space Science Reviews* **134**, 93–118 (2008). doi:10.1007/s11214-008-9311-x
- A. Finoguenov, C.L. Sarazin, K. Nakazawa, D.R. Wik, T.E. Clarke, XMM-Newton Observation of the Northwest Radio Relic Region in A3667. *Astrophys. J.* **715**, 1143–1151 (2010). doi:10.1088/0004-637X/715/2/1143
- D.C. Fox, A. Loeb, Do the Electrons and Ions in X-Ray Clusters Share the Same Temperature? *Astrophys. J.* **491**, 459–466 (1997). doi:10.1086/305007
- S.R. Furlanetto, A. Loeb, Intergalactic Magnetic Fields from Quasar Outflows. *Astrophys. J.* **556**, 619–634 (2001)
- S. Gabici, P. Blasi, Nonthermal Radiation from Clusters of Galaxies: The Role of Merger Shocks in Particle Acceleration. *Astrophys. J.* **583**, 695–705 (2003). doi:10.1086/345429
- M.R. George, A.C. Fabian, J.S. Sanders, A.J. Young, H.R. Russell, X-ray observations of the galaxy cluster PKS0745-191: to the virial radius, and beyond. *Mon. Not. Royal Astron. Soc.* **395**, 657–666 (2009). doi:10.1111/j.1365-2966.2009.14547.x
- S. Giacintucci, T. Venturi, G. Macario, D. Dallacasa, G. Brunetti, M. Markevitch, R. Cassano, S. Bardelli, R. Athreya, Shock acceleration as origin of the radio relic in A 521? *Astron. Astrophys.* **486**, 347–358 (2008). doi:10.1051/0004-6361/200809459
- G. Giovannini, L. Feretti, C. Stanghellini, The Coma cluster radio source 1253 + 275, revisited. *Astron. Astrophys.* **252**, 528–537 (1991)
- G. Giovannini, A. Bonafede, L. Feretti, F. Govoni, M. Murgia, The diffuse radio filament in the merging system ZwCl 2341.1+0000. *Astron. Astrophys.* **511**, 5 (2010). doi:10.1051/0004-6361/200913983
- F. Govoni, L. Feretti, G. Giovannini, H. Böhringer, T.H. Reiprich, M. Murgia, Radio and X-ray diffuse emission in six clusters of galaxies. *Astron. Astrophys.* **376**, 803–819 (2001). doi:10.1051/0004-6361:20011016
- M. Hoeft, M. Brüggen, Radio signature of cosmological structure formation shocks. *Mon. Not. Royal Astron. Soc.* **375**, 77–91 (2007). doi:10.1111/j.1365-2966.2006.11111.x
- M. Hoeft, M. Brüggen, G. Yepes, S. Gottlöber, A. Schwöpe, Diffuse radio emission from clusters in the MareNostrum Universe simulation. *Mon. Not. Royal Astron. Soc.* **391**, 1511–1526 (2008). doi:10.1111/j.1365-2966.2008.13955.x
- F.C. Jones, D.C. Ellison, The plasma physics of shock acceleration. *Space Science Reviews* **58**, 259–346 (1991). doi:10.1007/BF01206003
- H. Kang, T.W. Jones, Self-similar evolution of cosmic-ray-modified quasi-parallel plane shocks. *Astroparticle Physics* **28**, 232–246 (2007). doi:10.1016/j.astropartphys.2007.05.007
- H. Kang, D. Ryu, T.W. Jones, Cluster Accretion Shocks as Possible Acceleration Sites for Ultra-High-Energy Protons below the Greisen Cutoff. *Astrophys. J.* **456**, 422 (1996). doi:10.1086/176666
- H. Kang, D. Ryu, T.W. Jones, Self-Similar Evolution of Cosmic-Ray Modified Shocks: The Cosmic-Ray Spectrum. *Astrophys. J.* **695**, 1273–1288 (2009). doi:10.1088/0004-637X/695/2/1273
- H. Kang, D. Ryu, R. Cen, J.P. Ostriker, Cosmological Shock Waves in the Large-Scale Structure of the Universe: Nongravitational Effects. *Astrophys. J.* **669**, 729–740 (2007). doi:10.1086/521717
- T.N. Kato, H. Takabe, Nonrelativistic collisionless shocks in weakly magnetized electron-ion plasmas: two-dimensional particle-in-cell simulation of perpendicular shock. ( 2010)
- J.C. Kempner, E.L. Blanton, T.E. Clarke, T.A. Enßlin, M. Johnston-Hollitt, L. Rudnick, Conference Note: A Taxonomy of Extended Radio Sources in Clusters

- of Galaxies, in *The Riddle of Cooling Flows in Galaxies and Clusters of galaxies*, ed. by T. Reiprich, J. Kempner, N. Soker, 2004, p. 335
- U. Keshet, E. Waxman, Energy Spectrum of Particles Accelerated in Relativistic Collisionless Shocks. *Physical Review Letters* **94**(11), 111102 (2005). doi:10.1103/PhysRevLett.94.111102
- U. Keshet, E. Waxman, A. Loeb, V. Springel, L. Hernquist, Gamma Rays from Intergalactic Shocks. *Astrophys. J.* **585**, 128–150 (2003). doi:10.1086/345946
- R.A. Krivonos, A.A. Vikhlinin, M.L. Markevitch, M.N. Pavlinsky, A Possible Shock Wave in the Intergalactic Medium of the Cluster of Galaxies A754. *Astronomy Letters* **29**, 425–428 (2003). doi:10.1134/1.1589859
- G.F. Krymskii, A regular mechanism for the acceleration of charged particles on the front of a shock wave. *Akademiia Nauk SSSR Doklady* **234**, 1306–1308 (1977)
- R.M. Kulsrud, R. Cen, J.P. Ostriker, D. Ryu, The Protogalactic Origin for Cosmic Magnetic Fields. *Astrophys. J.* **480**, 481 (1997)
- A. Lazarian, Enhancement and Suppression of Heat Transfer by MHD Turbulence. *Astrophys. J. Lett.* **645**, 25–28 (2006). doi:10.1086/505796
- M. Lueker, C.L. Reichardt, K.K. Schaffer, O. Zahn, P.A.R. Ade, K.A. Aird, B.A. Benson, L.E. Bleem, J.E. Carlstrom, C.L. Chang, H. Cho, T.M. Crawford, A.T. Crites, T. de Haan, M.A. Dobbs, E.M. George, N.R. Hall, N.W. Halverson, G.P. Holder, W.L. Holzapfel, J.D. Hrubes, M. Joy, R. Keisler, L. Knox, A.T. Lee, E.M. Leitch, J.J. McMahon, J. Mehl, S.S. Meyer, J.J. Mohr, T.E. Montroy, S. Padin, T. Plagge, C. Pryke, J.E. Ruhl, L. Shaw, E. Shirokoff, H.G. Spieler, B. Stalder, Z. Staniszewski, A.A. Stark, K. Vanderlinde, J.D. Vieira, R. Williamson, Measurements of Secondary Cosmic Microwave Background Anisotropies with the South Pole Telescope. *Astrophys. J.* **719**, 1045–1066 (2010). doi:10.1088/0004-637X/719/2/1045
- M.A. Malkov, L. O’C Drury, Nonlinear theory of diffusive acceleration of particles by shock waves. *Reports on Progress in Physics* **64**, 429–481 (2001). doi:10.1088/0034-4885/64/4/201
- M. Markevitch, The L X-T Relation and Temperature Function for Nearby Clusters Revisited. *Astrophys. J.* **504**, 27 (1998). doi:10.1086/306080
- M. Markevitch, A.H. Gonzalez, L. David, A. Vikhlinin, S. Murray, W. Forman, C. Jones, W. Tucker, A Textbook Example of a Bow Shock in the Merging Galaxy Cluster 1E 0657-56. *Astrophys. J. Lett.* **567**, 27–31 (2002). doi:10.1086/339619
- M. Markevitch, F. Govoni, G. Brunetti, D. Jerius, Bow Shock and Radio Halo in the Merging Cluster A520. *Astrophys. J.* **627**, 733–738 (2005). doi:10.1086/430695
- M.V. Medvedev, L.O. Silva, M. Fiore, R.A. Fonseca, W.B. Mori, Generation of Magnetic Fields in Cosmological Shocks. *Journal of Korean Astronomical Society* **37**, 533–541 (2004)
- R. Mewe, Ionization of hot plasmas., in *NATO ASIC Proc. 300: Physical Processes in Hot Cosmic Plasmas*, ed. by W. Brinkmann, A. C. Fabian, & F. Giovannelli, 1990, pp. 39–65
- E.T. Million, S.W. Allen, Chandra measurements of non-thermal-like X-ray emission from massive, merging, radio halo clusters. *Mon. Not. Royal Astron. Soc.* **399**, 1307–1327 (2009). doi:10.1111/j.1365-2966.2009.15359.x
- F. Miniati, D. Ryu, H. Kang, T.W. Jones, R. Cen, J.P. Ostriker, Properties of Cosmic Shock Waves in Large-Scale Structure Formation. *Astrophys. J.* **542**, 608–621 (2000). doi:10.1086/317027
- F. Miniati, D. Ryu, H. Kang, T.W. Jones, Cosmic-Ray Protons Accelerated at Cosmological Shocks and Their Impact on Groups and Clusters of Galaxies. *Astrophys. J.* **559**, 59–69 (2001). doi:10.1086/322375
- S.M. Molnar, N. Hearn, Z. Haiman, G. Bryan, A.E. Evrard, G. Lake, Accretion Shocks in Clusters of Galaxies and Their SZ Signature from Cosmological Simulations. *Astrophys. J.* **696**, 1640–1656 (2009). doi:10.1088/0004-637X/696/2/1640
- D. Nagai, E. Lau, Gas Clumping in the Outskirts of Lambda-CDM Clusters. (2011)
- J. Niemiec, M. Ostrowski, Cosmic-Ray Acceleration at Relativistic Shock Waves with a “Realistic” Magnetic Field Structure. *Astrophys. J.* **610**, 851–867

- (2004). doi:10.1086/421730
- C.A. Norman, D.B. Melrose, A. Achterberg, The Origin of Cosmic Rays above 10 18.5 eV. *Astrophys. J.* **454**, 60 (1995). doi:10.1086/176465
- S. Paul, L. Iapichino, F. Miniati, J. Bagchi, K. Mannheim, Evolution of shocks and turbulence in major cluster mergers. ( 2010)
- V. Petrosian, A.M. Bykov, Particle Acceleration Mechanisms. *Space Science Reviews* **134**, 207–227 (2008). doi:10.1007/s11214-008-9315-6
- V. Petrosian, A. Bykov, Y. Rephaeli, Nonthermal Radiation Mechanisms. *Space Science Reviews* **134**, 191–206 (2008). doi:10.1007/s11214-008-9327-2
- C. Pfrommer, T.A. Enßlin, V. Springel, M. Jubelgas, K. Dolag, Simulating cosmic rays in clusters of galaxies - I. Effects on the Sunyaev-Zel'dovich effect and the X-ray emission. *Mon. Not. Royal Astron. Soc.* **378**, 385–408 (2007). doi:10.1111/j.1365-2966.2007.11732.x
- G.W. Pratt, H. Böhringer, J.H. Croston, M. Arnaud, S. Borgani, A. Finoguenov, R.F. Temple, Temperature profiles of a representative sample of nearby X-ray galaxy clusters. *Astron. Astrophys.* **461**, 71–80 (2007). doi:10.1051/0004-6361:20065676
- G.W. Pratt, M. Arnaud, R. Piffaretti, H. Böhringer, T.J. Ponman, J.H. Croston, G.M. Voit, S. Borgani, R.G. Bower, Gas entropy in a representative sample of nearby X-ray galaxy clusters (REXCESS): relationship to gas mass fraction. *Astron. Astrophys.* **511**, 85 (2010). doi:10.1051/0004-6361/200913309
- C.E. Rakowski, J.M. Laming, P. Ghavamian, The Heating of Thermal Electrons in Fast Collisionless Shocks: The Integral Role of Cosmic Rays. *Astrophys. J.* **684**, 348–357 (2008). doi:10.1086/590245
- T.H. Reiprich, D.S. Hudson, Y. Zhang, K. Sato, Y. Ishisaki, A. Hoshino, T. Ohashi, N. Ota, Y. Fujita, Suzaku measurement of Abell 2204's intracluster gas temperature profile out to 1800 kpc. *Astron. Astrophys.* **501**, 899–905 (2009). doi:10.1051/0004-6361/200810404
- Y. Rephaeli, J. Nevalainen, T. Ohashi, A.M. Bykov, Nonthermal Phenomena in Clusters of Galaxies. *Space Science Reviews* **134**, 71–92 (2008). doi:10.1007/s11214-008-9314-7
- K. Roettiger, J.O. Burns, J.M. Stone, A Cluster Merger and the Origin of the Extended Radio Emission in Abell 3667. *Astrophys. J.* **518**, 603–612 (1999). doi:10.1086/307327
- S. Rosswog, M. Bruggen, *Introduction to High-Energy Astrophysics* 2007
- H.J.A. Röttgering, M.H. Wieringa, R.W. Hunstead, R.D. Ekers, The extended radio emission in the luminous X-ray cluster A3667. *Mon. Not. Royal Astron. Soc.* **290**, 577–584 (1997)
- H.J.A. Röttgering, M.H. Wieringa, R.W. Hunstead, R.D. Ekers, The extended radio emission in the luminous X-ray cluster A3667. *Mon. Not. Royal Astron. Soc.* **290**, 577–584 (1997)
- H. Röttgering, I. Snellen, G. Miley, J.P. de Jong, R.J. Hanisch, R. Perley, VLA observations of the rich X-ray cluster Abell 2256. *Astrophys. J.* **436**, 654–668 (1994). doi:10.1086/174940
- H.R. Russell, J.S. Sanders, A.C. Fabian, S.A. Baum, M. Donahue, A.C. Edge, B.R. McNamara, C.P. O'Dea, Chandra observation of two shock fronts in the merging galaxy cluster Abell 2146. *Mon. Not. Royal Astron. Soc.* , ( 2010). doi:10.1111/j.1365-2966.2010.16822.x
- D. Ryu, H. Kang, E. Hallman, T.W. Jones, Cosmological Shock Waves and Their Role in the Large-Scale Structure of the Universe. *Astrophys. J.* **593**, 599–610 (2003). doi:10.1086/376723
- D. Ryu, H. Kang, J. Cho, S. Das, Turbulence and Magnetic Fields in the Large-Scale Structure of the Universe. *Science* **320**, 909 (2008). doi:10.1126/science.1154923
- J.S. Sanders, A.C. Fabian, R.K. Smith, J.R. Peterson, A direct limit on the turbulent velocity of the intracluster medium in the core of Abell 1835 from XMM-Newton. *Mon. Not. Royal Astron. Soc.* **402**, 11–15 (2010). doi:10.1111/j.1745-3933.2009.00789.x
- A.A. Schekochihin, S.C. Cowley, R.M. Kulsrud, G.W. Hammett, P. Sharma, Plasma Instabilities and Magnetic Field Growth in Clusters of Galaxies. *Astrophys. J.*



- 629**, 139–142 (2005). doi:10.1086/431202
- S.J. Schwartz, M.F. Thomsen, S.J. Bame, J. Stansberry, Electron heating and the potential jump across fast mode shocks. *JGR* **93**, 12923–12931 (1988)
- L.D. Shaw, D. Nagai, S. Bhattacharya, E.T. Lau, Impact of Cluster Physics on the Sunyaev-Zel'dovich Power Spectrum. *Astrophys. J.* **725**, 1452–1465 (2010). doi:10.1088/0004-637X/725/2/1452
- A. Simionescu, E. Roediger, P.E.J. Nulsen, M. Brüggen, W.R. Forman, H. Böhringer, N. Werner, A. Finoguenov, The large-scale shock in the cluster of galaxies Hydra A. *Astron. Astrophys.* **495**, 721–732 (2009). doi:10.1051/0004-6361/200811071
- A. Simionescu, S.W. Allen, A. Mantz, N. Werner, Y. Takei, R.G. Morris, A.C. Fabian, J.S. Sanders, P.E.J. Nulsen, M.R. George, G.B. Taylor, Baryons at the Edge of the X-ray Brightest Galaxy Cluster. ( 2011)
- L. Sironi, A. Spitkovsky, Particle Acceleration in Relativistic Magnetized Collisionless Electron-Ion Shocks. ( 2010)
- S.W. Skillman, B.W. O'Shea, E.J. Hallman, J.O. Burns, M.L. Norman, Cosmological Shocks in Adaptive Mesh Refinement Simulations and the Acceleration of Cosmic Rays. *Astrophys. J.* **689**, 1063–1077 (2008). doi:10.1086/592496
- A. Spitkovsky, Particle Acceleration in Relativistic Collisionless Shocks: Fermi Process at Last? *Astrophys. J. Lett.* **682**, 5–8 (2008). doi:10.1086/590248
- R.J. van Weeren, H.J.A. Röttgering, M. Brüggen, A. Cohen, A search for steep spectrum radio relics and halos with the GMRT. *Astron. Astrophys.* **508**, 75–92 (2009a). doi:10.1051/0004-6361/200912501
- R.J. van Weeren, H.J.A. Röttgering, J. Bagchi, S. Raychaudhury, H.T. Intema, F. Miniati, T.A. Enßlin, M. Markevitch, T. Erben, Radio observations of ZwCl 2341.1+0000: a double radio relic cluster. *Astron. Astrophys.* **506**, 1083–1094 (2009b). doi:10.1051/0004-6361/200912287
- R.J. van Weeren, H.J.A. Röttgering, J. Bagchi, S. Raychaudhury, H.T. Intema, F. Miniati, T.A. Enßlin, M. Markevitch, T. Erben, Radio observations of ZwCl 2341.1+0000: a double radio relic cluster. *Astron. Astrophys.* **506**, 1083–1094 (2009c). doi:10.1051/0004-6361/200912287
- R.J. van Weeren, H.J.A. Röttgering, M. Brüggen, M. Hoeft, Particle Acceleration on Megaparsec Scales in a Merging Galaxy Cluster. *Science* **330**, 347 (2010). doi:10.1126/science.1194293
- R.J. van Weeren, H.J.A. Röttgering, M. Brüggen, M. Hoeft ( 2011)
- F. Vazza, G. Brunetti, C. Gheller, Shock waves in Eulerian cosmological simulations: main properties and acceleration of cosmic rays. *Mon. Not. Royal Astron. Soc.* **395**, 1333–1354 (2009a). doi:10.1111/j.1365-2966.2009.14691.x
- F. Vazza, G. Brunetti, A. Kritsuk, R. Wagner, C. Gheller, M. Norman, Turbulent motions and shocks waves in galaxy clusters simulated with adaptive mesh refinement. *Astron. Astrophys.* **504**, 33–43 (2009b). doi:10.1051/0004-6361/200912535
- F. Vazza, G. Brunetti, C. Gheller, R. Brunino, Massive and refined: A sample of large galaxy clusters simulated at high resolution. I: Thermal gas and properties of shock waves. *New Astronomy* **15**, 695–711 (2010). doi:10.1016/j.newast.2010.05.003
- T. Venturi, S. Giacintucci, G. Brunetti, R. Cassano, S. Bardelli, D. Dallacasa, G. Setti, GMRT radio halo survey in galaxy clusters at  $z = 0.2-0.4$ . I. The REFLEX sub-sample. *Astron. Astrophys.* **463**, 937–947 (2007). doi:10.1051/0004-6361/20065961
- A. Vikhlinin, M. Markevitch, S.S. Murray, C. Jones, W. Forman, L. Van Speybroeck, Chandra Temperature Profiles for a Sample of Nearby Relaxed Galaxy Clusters. *Astrophys. J.* **628**, 655–672 (2005). doi:10.1086/431142
- A. Vladimirov, D.C. Ellison, A. Bykov, Nonlinear Diffusive Shock Acceleration with Magnetic Field Amplification. *Astrophys. J.* **652**, 1246–1258 (2006). doi:10.1086/508154
- A.E. Vladimirov, A.M. Bykov, D.C. Ellison, Turbulence Dissipation and Particle Injection in Nonlinear Diffusive Shock Acceleration with Magnetic Field Amplification. *Astrophys. J.* **688**, 1084–1101 (2008). doi:10.1086/592240

- 
- C. Vogt, T.A. Enßlin, A Bayesian view on Faraday rotation maps Seeing the magnetic power spectra in galaxy clusters. *Astron. Astrophys.* **434**, 67–76 (2005). doi:10.1051/0004-6361:20041839
- K. Wong, C.L. Sarazin, Effects of the Non-Equipartition of Electrons and Ions in the Outskirts of Relaxed Galaxy Clusters. *Astrophys. J.* **707**, 1141–1159 (2009). doi:10.1088/0004-637X/707/2/1141
- Y.B. Zeldovich, A hypothesis, unifying the structure and the entropy of the Universe. *Mon. Not. Royal Astron. Soc.* **160**, 1 (1972)
- V.N. Zirakashvili, V.S. Ptuskin, H.J. Völk, Modeling Bell's Nonresonant Cosmic-Ray Instability. *Astrophys. J.* **678**, 255–261 (2008). doi:10.1086/529579